Master Thesis, Department of Geosciences

An experimental study to determine the potential of synthetic pyroaurite to remove Pb(II) from aqueous solutions

Anum Irfan

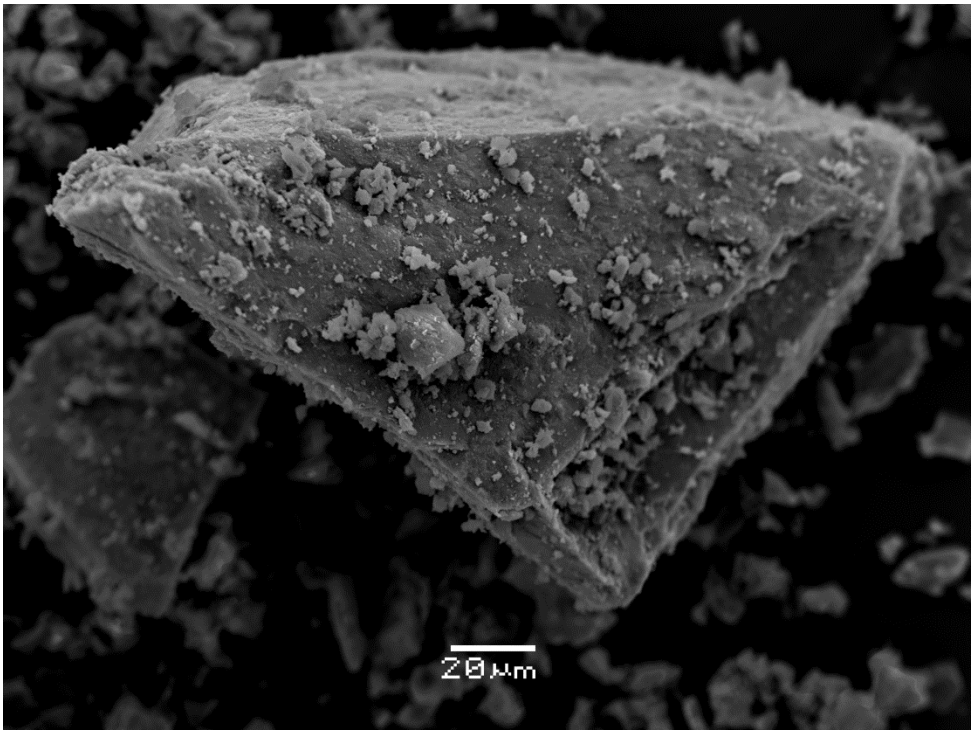

UNIVERSITY OF OSLO
FACULTY OF MATHEMATICS AND NATURAL SCIENCES

An experimental study to determine the potential of synthetic pyroaurite to remove Pb(II) from aqueous solutions

Anum Irfan

Master Thesis in Geosciences
Discipline: Environmental Geology and Geohazards
Department of Geosciences

Faculty of Mathematics and Natural Sciences

University of Oslo

August 2014

Supervisor(s): Dr. Helge Hellevang, Prof.PerAagaard, Prof.Håkon O. Austrheim

This work is published digitally through DUO – DigitaleUtgivelservedUiO

http://www.duo.uio.no

It is also catalogued in BIBSYS (http://www.bibsys.no/english)

Acknowledgements

There are many people I want to acknowledge for their contribution, support and interest for this project. First and foremost I want to thank all my supervisors for making this project possible. I am very grateful to Dr. Helge Hellevang for his support, guidance and useful suggestions throughout this duration. It has been such an interesting and rewarding work which can actually contributes for solving environmental issue.

I am very thankful to my co-supervisors Prof. Per Aagaard and Prof. Håkon Austrheim for proposing this thesis and for their affection and continuous guidance. All of them helped me to solve the issues I encountered during this work. This thesis would have never been accomplished without their support. The most important thing they taught me is not only limited to geochemistry concepts but the way to think and solve problems independently as well as cooperatively.

I thank all the technical and non-teaching staff of the Department of Geosciences. I particularly want to thank Maarten Aerets, Muriel Erambert, Siri Lene Simonsen, Berit Løken, and Mufak Naoroz for their help and cooperation during laboratory work.

I would like to express my appreciation to Oluwakemi Yetunde Ogebule, Aatisha Mahajan from our department and my fellow student Uzair Naqvi for spending time on reviewing my thesis and giving valuable feedback. Very special thanks to Beyene Girma Haile for useful discussions and positive criticism which enabled me to improve this work.

I am very grateful to my husband, who always helped and encouraged me throughout my academic years. To my beloved parents for their love and prayers especially my father who has always believed in me.

Last but not least, I am very thankful to University of Oslo, especially the Department of Geosciences for giving me the opportunity to be a part of this leading institute.

Abstract

The aim of the thesis was to examine the potential of synthetic pyroaurite to remove lead(II) from contaminated water. This study was based upon column experiments run in duplicate at room temperature.

Heavy metals, many being toxic and bio-accumulative in nature pose a major threat to soil water environment and human health. Lead(II) is among one of the environmental pollutant which is known to be toxic to human health if present in significant amount in waters. To remove such toxic metals from waters, many methods have been developed. The same problem has been addressed in this study. A low cost Mg and Fe based carbonate hydroxide i.e. pyroaurite was synthesized in the laboratory and the removal of Pb^{2+} from $Pb(NO_3)_2$ solution by sorption was investigated. This was done by performing column experiments.

The prepared synthetic material was characterized first using XRD and SEM to observe the composition and crystal structure of the material. Poorly crystallized material was formed in the laboratory while presence of a pyroaurite-like compound was confirmed by XRD analysis. The fine-grained synthesized material was mixed with a natural sand to improve the flow properties of the packed column. A solution of 5.8 ppm $Pb(NO_3)_2$ was pumped through the column at a rate of 1.25 ml/hr. The effluent was sampled with every 20 or 30 minutes. The two duplicate experiments were run respectively for 8 and 22 days.

The concentration of Pb^{2+} was analysed in the effluent using ICP-MS. Very low concentration of lead(II) was detected in the outlet samples as compared to the incoming Pb(II) concentration into the column, revealing that most of the lead(II) is captured inside the column. On the average 99% of the injected Pb(II) was removed. The effluent concentration was well below recommended drinking water standard by World health organization (WHO).The reacted solid column material was analysed by XRD and SEM. The XRD examination did not reveal presence of a secondary Pb-phase in the reacted samples due to traceable amounts of Pb(II) inside the column material. On the other hand, SEM analysis revealed the presence of Pb(II) in few samples from reacted material. The appropriate mechanism of sorption by which lead(II) is taken up by pyroaurite-like material is not clear, though adsorption and precipitation are considered to be the major mechanisms.

It is suspected that major part of lead(II) is precipitated on the synthetic pyroaurite material, as Pb(II) was found in the form of small particles in some of the samples examined. Some traces of lead(II) may also be scavenged by adsorption, but no desorption experiments were carried out to verify it. The results indicated that the precipitates were formed either as lead carbonates or lead oxides. Observations and calculations have showed that about 99% of Pb(II) is taken up by pyroaurite-like material. The results suggested that synthetic pyroaurite has potential to remove Pb^{2+} from aqueous solutions and therefore can be a good candidate for the purification of contaminated waters.

Contents

List of Abbreviations

BSEI	Back scattered electron image
EDS	Energy Dispersive Spectrometer
EMP	Electron Microprobe
IC	Ion Chromatography
ICP-MS	Inductively Coupled Plasma Mass Spectrometry
Pb(II)	Lead(II)
$Pb(NO_3)_2$	Lead(II) Nitrate
ppm	Parts per million
ppb	Parts per billion
SEI	Secondary Electron Image
SEM	Scanning Electron Microscope
XRD	X-Ray Diffraction

List of Figures

List of Tables

1. Introduction

Pollution by heavy metals is one of the major environmental issues these days. Many industries are known for the discharge of heavy metals as industrial effluents into the environment. Industries including tanneries, metallurgic, mineral processing, electroplating and dyeing industries are usually responsible for the production of heavy metal wastes (Jaiswal and Chattopadhyaya, 2011).

Due to the toxic nature and bio-accumulating property of heavy metals, they play a major role in polluting soil and water environment and thus, can cause serious health problems (Setshedi et al., 2012). Heavy metals can be taken up by aquatic organisms thereafter, accumulating in their bodies (Rashed, 2001).

Usually heavy metals are known to have densities greater than 5 g/cm^3. Among heavy metals, cadmium, lead and mercury are known to have serious impacts on human health upon exposure to them. Heavy metals can enter into the environment through various routes such as atmospheric emissions from combustion and extraction processes, run-off from industries which pollute surface waters and leach through soils thereby polluting ground water (Järup, 2003). Smelting and mining industries along with storage battery-manufacturing industries are largely responsible for the discharge of lead in waste waters which disturb aquatic life (Rashed, 2001).

According to World Health Organization, more than 3.5 million people die every year due to consumption of contaminated water. In addition, pollution by heavy metals makes the condition more severe (Jayakumar et al., 2010). This makes it necessary to remove these metal ions from water. Different methods are used widely for the removal of the heavy metal ions from wastewaters (Fu and Wang, 2011). These methods include ion-exchange, chemical precipitation, membrane filtration, reverse osmosis (Naeem et al., 2009; Naiya et al., 2009). Many of these methods are known to be costly yet, not highly effective. They also have other disadvantages including production, disposal problems of secondary wastes and incomplete removal of metal ions (Diouf et al., 2011; Egila et al., 2011). Aluminium salts and activated carbon have been used worldwide as coagulants in water treatment for the removal of colour, odour, turbidity, organic matter, and chemicals. These are known for their effectiveness and

efficiency. Recently, it was revealed that human exposure to aluminium is considered a risk to the development or the acceleration of Alzheimer's disease (WHO, 2011).

Lead(II) is the most common environmental pollutant found in soils. It does not have any biological role but is likely to be toxic to micro-organisms present in soils (Sobolev and Begonia, 2008). Lead, when present in high amounts in water, is known to have acute toxicity in humans. Intake of lead(II) even at low concentrations can affect human health (Adelekan and Abegunde, 2011). Soil pollution by dilute lead is commonly found at lead-related industrial sites (Reed et al., 1996) and also in drinking water which is supplied via lead-made pipes (Seida et al., 2001). Removal of lead from waste water is highly becoming a major environmental concern because of its impacts on health and environment.

1.1. Project description and objectives

The overall goal of the study is to evaluate the potential of synthetic pyroaurite mineral as an adsorbent for the removal of dilute lead(II) from water.

The first step is to synthesize the pyroaurite-like compound and then perform sorption experiment of Pb(II) and column experiments with laboratory prepared pyroaurite. The synthetic material is then characterized and analysed in relation to its composition and structure using analytical techniques such as X-ray diffraction (XRD) and scanning electron microscopy (SEM).

After running the column experiments, concentration of lead in the effluent samples are analysed using inductively coupled plasma mass spectrometry (ICP-MS). Then the difference in concentration of Pb(II) from the incoming solution and the effluent samples is evaluated in order to estimate how much lead is taken up by the pyroaurite mineral.

Finally to examine any significant changes in the pyroaurite material and to evaluate the mechanisms responsible for lead uptake, XRD and SEM examinations of the reacted materials are carried out.

2. Theoretical background

Heavy metal pollution has become one of the most serious environmental problems these days. The treatment of heavy metals is of very much concern due to their resistance and perseverance in the environment. Heavy metals even at low doses can cause serious health problems, including reduced growth and development, cancer, organ damage, nervous system damage, and in extreme cases, death. Exposure to some metals, such as lead and mercury, may also cause development of autoimmunity, in which a person's immune system attacks its own cells. This can lead to joint damage and diseases of the kidneys, circulatory system, nervous system, and damage of the fetal brain. At higher doses, heavy metals can cause irreversible brain damage. Children may receive higher doses of metals from food than adults, since they consume more food for their body weight than adults. Wastewater regulations were established to minimize human and environmental exposure to hazardous chemicals. This includes limits on the types and concentration of heavy metals that may be present in the discharged wastewater (Barakat, 2011). Many industrial wastewater streams contain heavy metals that must be removed prior to water discharge or recycling (Kim et al., 2001). The heavy metals are, for the most part, responsive to practical treatment methods for water cleansing and metal recovery processes (Dean et al., 1972). In the recent years, various approaches considered for heavy metal removal from wastewater have been extensively studied for the development of cheaper and more effective technologies, both to decrease the amount of produced wastewater and to improve the quality of the treated discharge. The most commonly applied treatment methods are chemical precipitation, ion-exchange, adsorption, membrane filtration, coagulation flocculation, flotation and electrochemical (Kim et al., 2001; Igwe et al., 2006; Barakat, 2011). Though adsorption and precipitation remain the most widely used and popular methods for the removal of heavy metal ions but flotation and membrane filtration are also attaining increasing attention these days (Blöcher et al., 2003).

In this chapter, a brief introduction will be presented to commonly used treatment techniques for the removal of heavy metals from wastewaters with special emphasis and focus on chemical precipitation and adsorptions techniques that we have used in our study.

2.1. Ion-exchange

Ion-exchange processes are widely applied to remove heavy metals from wastewater. Ion-exchange processes have many advantages due to their high removal efficiency, high treatment capacity, and fast kinetics. Ion exchanger is a solid capable of exchanging either cations or anions with the metal from the wastewater (Barakat, 2011). Both natural and synthetic solids are used as ion-exchange resins. Although naturally occurring zeolites and silicate minerals, have been widely used to remove heavy metal from aqueous solutions due to their low cost and high abundance (Fu and Wang, 2011), but synthetic resins are commonly preferred over natural resins in ion-exchange processes, as they are more effective to remove heavy metals from the surrounding solution (Alyüz and Veli, 2009).The most commonly used cation exchangers are strongly acidic resins with sulfonic acid groups (-SO_3H) and weakly acid resins with carboxylic acid groups (-COOH). When the solution containing heavy metals are passed through the cations column, heavy metal ions are exchanged for the hydrogen ions on the resin (Fu and Wang, 2011).

$$nR - SO_3H + M^{n+} \rightarrow (R - SO_3^-)_n M^{n+} + nH^+ \quad (2\text{-}1)$$

$$nR - COOH + M^{n+} \rightarrow (R - COO^-)_n M^{n+} + nH^+ \quad (2\text{-}2)$$

where (–RSO_3–) and M are the anionic group attached to the ion exchange resin and the metal cation, respectively, while n is the coefficient of the reaction component, which depends on the oxidation state of metal ions (Dabrowski et al., 2004).

The removal of heavy metal ions by ion-exchange resins is affected by certain variables such as pH, temperature, initial metal concentration, and contact time. Ionic charge also plays an important role in the removal of heavy metal ions through ion-exchange process (Gode and Pehlivan, 2006).

2.2. Membrane filtration

Membrane filtration technologies with different types of membranes have shown great potential for heavy metal removal for their high efficiency, easy operation, and space saving characteristics. Filtration plays an important role in physical processes of wastewater treatment methods. The membranes are usually synthetic organic materials and are normally laminated. When set into pressurized ducts, these elements allow continuous flow, with the filtrate passing into parallel chambers. The membrane consists of semi-permeable membranes

which act fundamentally as molecular sieves allowing soluble compounds of various molecular size ranges to pass through their pores (Dean et al., 1972). Depending on the size of the particle that can be retained, various types of membrane techniques such as ultrafiltration, reverse osmosis, nanofiltration and electrodialysis can be used to remove heavy metals from the wastewater (Barakat, 2011; Fu and Wang, 2011).

2.3. Flotation

Flotation is another widely used wastewater treatment these days. Dissolved air flotation, ion floatation and precipitation floatation are the main floatation processes used for removing heavy metal ions from the wastewater solutions using bubble attachment (Fu and Wang, 2011). The general principle in flotation is to allow micro-bubbles of air to attach to the suspended particles in the water that form agglomerates with lower density than water, causing flocs to rise through the water and accumulating at the surface where they can be removed as sludge (Lundh et al., 2000).

2.4. Sorption

Sorption is a combined term used for absorption and adsorption. In absorption the chemical sinks into the solid surface while in adsorption, the chemical is attached to the surface of the solid (Appelo and Postma, 2005). Sorption is actually a transfer of ions from solution to the solid phase through a group of processes which includes adsorption and precipitation reactions (Barakat, 2011). Sorption process is highly dependent on experimental conditions like concentration of metals, competing ions and pH (Bailey et al., 1999). Adsorption and surface precipitation are examples of sorption. However, surface precipitation is not a part of adsorption. Surface precipitation results in the growth of a new solid phase which consists of 3 dimensional arrangement of repeating units (Sparks, 2003).

2.5. Adsorption

In recent years, adsorption has become one of the best alternative techniques for water treatment by removal of heavy metals, and the search has increased significantly for finding low-cost adsorbents that have metal-affinity (Leung et al., 2000). In the adsorption process, the chemical substance travels from aqueous phase to the solid surface and is bounded to the solid adsorbent surface by means of chemical or physical interactions (Kurniawan and Babel,

2003). In this way heavy metals can bind to the particular sorbent which may help in decreasing the mobility and leaching of toxic metals in soils and groundwater. Metal mobility also depends upon the physical and chemical properties of soil to determine its binding power. These properties include mineral composition, organic matter content of soil, clay fraction and pH (Stevenson, 1994; Kurniawan and Babel, 2003). It has been said that in soils, the solids which have a large surface area will have more tendency for adsorption. Capacity of a solid surface is also dependent upon the clay fraction of soils, organic matter content, clay minerals and oxides or hydroxides. Cation exchange capacity (CEC) is the term used to indicate the quantity of cations that are adsorbed per unit weight of mineral. Clay minerals and organic matter have high cation exchange capacity. It is associated with percentage of clay and organic carbon content (Appelo and Postma, 2005) as represented in the formula below:

$$\text{CEC (meq/kg)} = (\%\ \text{clay}) + 35.\ (\%\ \text{C})$$

Sorption is a reversible reaction as contaminant has an ability of sorption and desorption. As a contaminant has ability to sorb from aqueous phase to a solid phase likewise it can also desorb from the solid phase to the aqueous phase. These rates of sorption and desorption depends upon the concentration of sorbed contaminant and also on strength of bonding between contaminant and the surface. Some contaminants bound strongly to the surface while others are weakly bounded (Weiner, 2012).

Transport of contaminants is dependent on the sorption processes which can retard their mobility in groundwater. Assuming a linear sorption isotherm, retardation factor for movement of a contaminant can be explained by the following equation:

$$R = 1 + Kd$$

Here Kd is distribution coefficient which describes equilibrium conditions when rate of sorption and desorption are equal. This distribution coefficient is given by:

$$Kd = \frac{dq}{dc}$$

Kd is dimensionless, dq is the concentration of solute adsorbed on solid expressed in (mg/l), while dc shows the concentration of solute (mg/l) in the solution. If concentration of solute

adsorbed on the solid is equal to the concentration of solute in the solution, then ratio of Kd will be 1 (Appelo and Postma, 2005). Transport of contaminant in groundwater depends upon the value of Kd. If value of Kd is equal to zero, then the contaminant will not sorb to the soil and travels with the speed of groundwater, whereas if Kd is higher then the movement of contaminant will be retarded (Weiner, 2012).

2.6. Chemical precipitation

Chemical precipitation is the most generally applied treatment method, particularly where economic recovery is not a consideration and no complex chemical compounds are involved (Dean et al., 1972). Chemical precipitation is the widely used method for removing heavy metals from inorganic industrial waste discharge water. Chemical precipitation is usually favorable in basic environment (Wang et al., 2005). The most commonly used chemical precipitation approach is hydroxide precipitation in which the metal is precipitated out in the form of hydroxide from the aqueous media (Huisman et al., 2006). The mechanism for removal of heavy metal by means of chemical precipitation is as follows:

$$M^{2+} + 2(OH)^- \leftrightarrow M(OH)_2 \qquad (2\text{-}3)$$

Where M^{2+} is the dissolved heavy metal ion and $(OH)^-$ acts as a precipitant whereas, $M(OH)_2$ is the insoluble metal hydroxide (Wang et al., 2005). The precipitates can then be isolated from water by the process of flocculation or sedimentation (Baltpurvins et al., 1997).

Many research works have been done on heavy metal adsorption on negatively charged clay minerals. However, there are only a few studies which have focused for removal of metal cations on adsorbents which are positively charged like layered double hydroxides (Seida et al., 2001; Liang et al., 2009).

2.7. Layered double hydroxides (LDHs)

Layered double hydroxides (LDHs) minerals from hydrotalcite group, also known as anionic clays are used as catalysts for the removal of contaminants. This group includes both natural and synthetic layered minerals. They are used as adsorbent for removing inorganic contaminants by means of ion exchange or adsorption (Forano, 2004; Liang et al., 2009). The representative formula for LDHs is as given below:

$[M_{1-x}^{2+} M^{3+}_x OH)_2] [A^{n-}_{x/}n. m H2O]^{x-}$

Where M^{2+} and M^{3+} represents divalent and trivalent metal cations. A^{n-} is the anion for balancing the positive charge, x is the molar ratio of metal cations. Structure of LDHs consists of positively charged brucite sheets and this excess positive charge is equalized by insertion of anions in the interlayer hydrated region. These anions can be interchanged with other anions and thus, this property of anion exchange of LDHs makes them unique (Figure 2-1) (Liang et al., 2009). Studies on sorption of metal cations on LDHs are rare as compared to anion sorption. These double layered hydroxides are also found in the form of natural minerals like pyroaurite (Mg-Fe LDH), hydrotalcite (Mg-Al LDH) and takovite (Ni-Al LDH) usually having carbonates or occasionally chlorides as interlayer anions (Liang et al., 2013).

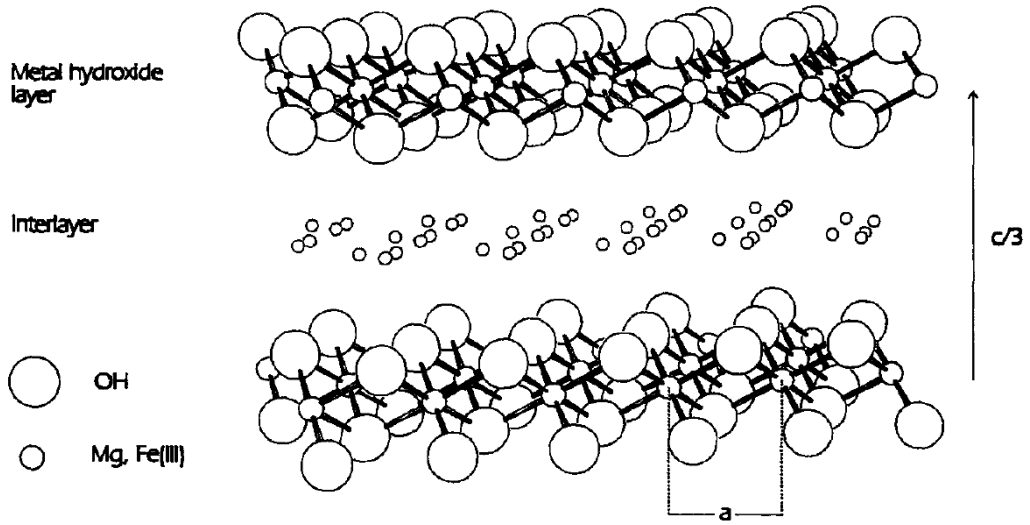

Figure 2-1: Illustration of Mg-Fe LDH structure after Allmann (1968).

According to Seida and Nakano (2000) adsorption of cations on LDHs usually increases with the increasing pH but in few cases LDHs have buffering pH effect. In adsorption process there is an interaction between solutes from aqueous media and solid surfaces which can be explained as surface complexation process. As ions in liquid solution form ion pairs or complexes likewise heavy metals also form metal complexes. These complexes are of two types i.e. inner sphere and outer sphere complexes (Burgess, 1999). In inner sphere complexes, chemical binding between metal ions and surface functional group takes place. It can also refer as specific adsorption. On the other hand, the outer sphere complexes takes place at a particular distance from the solid surface and are formed due to electrostatic binding between oppositely charged surface functional groups and metal ions (Figure 2-2) (Lützenkirchen, 2002; Liang et al., 2013).

Pyroaurite is an anionic clay (Miyata, 1983), that belongs to the hydrotalcite group of minerals with a general formula $(Mg_{(8-x)}Fe_x\ (OH)_{16})^{x+}\ (CO_3.yH_2O)^{x-}$. According to (Kruissink et al., 1981) x is found to be within the range 1.2-3.6. Koch (1998) has found extensive use of pyroaurite in catalysis and environmental chemistry to retain hazardous cations and anions. According to Reichle (1986), pyroaurite is also called clay type anion exchanger having a structure of layered double hydroxide, where (*x=3; y= 1*).

Seida and Nakano (2000) reported that pyroaurite-like compounds are non aluminium based compounds, which are effective in removal of humic substances and phosphate. These compounds show low dissolution in aqueous environment due to buffering pH effect. Through slight solubility of their hydroxides they could be capable in removing heavy metal cations. It also works efficiently in some water treatments as it establish a weak alkali environment due to dissolution by releasing metal hydroxides and cations which functions as coagulants (Seida and Nakano, 2000).

Pyroaurite is present in the weathering zone of the Feragen Ultramafic Complex, southeast Norway where it constitutes up to 10 modal wt% of the rock. It occurs typically in mm to cm thick veins together with hydrocarbonates (dypingite and nesqueonite). It may be zoned with colours ranging from yellowish (high x) to greyish (low x) (Beinlich and Austrheim, 2012). Typically the Fe rich core is replaced by a low Fe rim, but the reverse zoning is also present. There is an abrupt change in composition between the rim and the core resembling a replacement front. The content of Mn, as the desautelsite component ($Mg_6Mn_2(CO_3)(OH)_{16}4H_2O$), increases with increasing FeO; while the NiO content reaches the highest values (1.2 wt%) in the low Fe parts. At present pyroaurite used in environmental chemistry is produced by a synthesis as described by (Hansen and Taylor, 1990; Bruun Hansen and Koch, 1995).

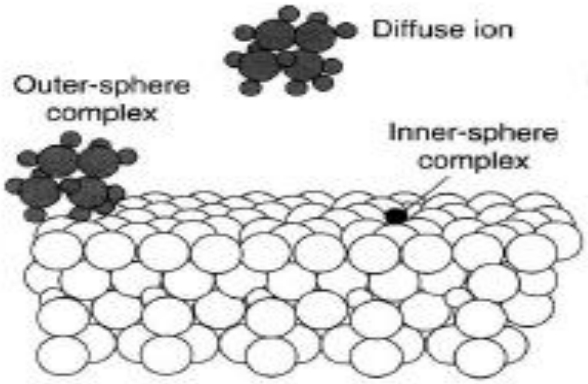

Figure 2-2: Illustration of a charged surface which represents outer and inner sphere complexes modified after Appelo and Postma (2005).

3. Materials and methods

This study is based on the laboratory work and analysis.

3.1. Preparation of pyroaurite-like compound

The following procedure from Seida et al. (2001) was used to synthesize pyroaurite-like compounds in the laboratory:

0.075 mol of $FeCl_3$ and 0.15mol of $MgCl_2$ salts were needed. In order to do so, the salts were weighed first.

$MgCl_2.6H_2O$ (molecular weight) = 203.30 g/mol × 0.15 = 30.5 gram;

$FeCl_3$ = 162,197 g/mol × 0.075 = 12.1647 gram

30.52 gram of magnesium chloride ($MgCl_2.6H_2O$) and 12.1645 gram of iron(III) chloride ($FeCl_3$) was dissolved into 200 ml of distilled water (millipore). After mixing the two salts into the distilled water, the beaker was placed on the magnetic stirrer. 10 wt% of NaOH (in aqueous form) was added then into the solution drop wise while pH of the solution was observed continuously. As we kept on adding the strong base sodium hydroxide (NaOH), the solution becomes thicker and thicker as seen in Figure 3-1b. The procedure continued until the solution reached pH of 13. The solution was then kept on stirrer for 24 hours at room temperature. Under this condition, carbon dioxide from the atmosphere diffuses into the alkaline solution. After 24 hours, the solution looked like brownish-orange slurry (Figure 3-1c).

The slurry was then filtered using Whatman filter papers to obtain the precipitates (Figure 3-2). Afterwards the precipitates were shaked and suspended in the deionized water. They were washed with the distilled water several times so that the residual chemicals would be washed out. The obtained precipitates were brownish in colour (Figure 3-3). After washing and removing water from the material, the precipitates were placed into the electric oven for drying at 110ºC for approximately 24 hours. Using agate mortar, the dried material was then crushed into smaller sized particles by hand and was used for further laboratory analysis.

Figure 3-1: Set up used for preparing the pyroaurite material in the laboratory. a) Initial solution of $FeCl_3$ and $MgCl_2$ before titration. b) The solution when titrated with NaOH at pH 9.0. c) The final prepared solution at pH 13.06 after titration.

Figure 3-2: Typical set-up in the laboratory for filtration. The filter is placed on the glass platform, then the solution is added and the distilled water is drawn using the vacuum.

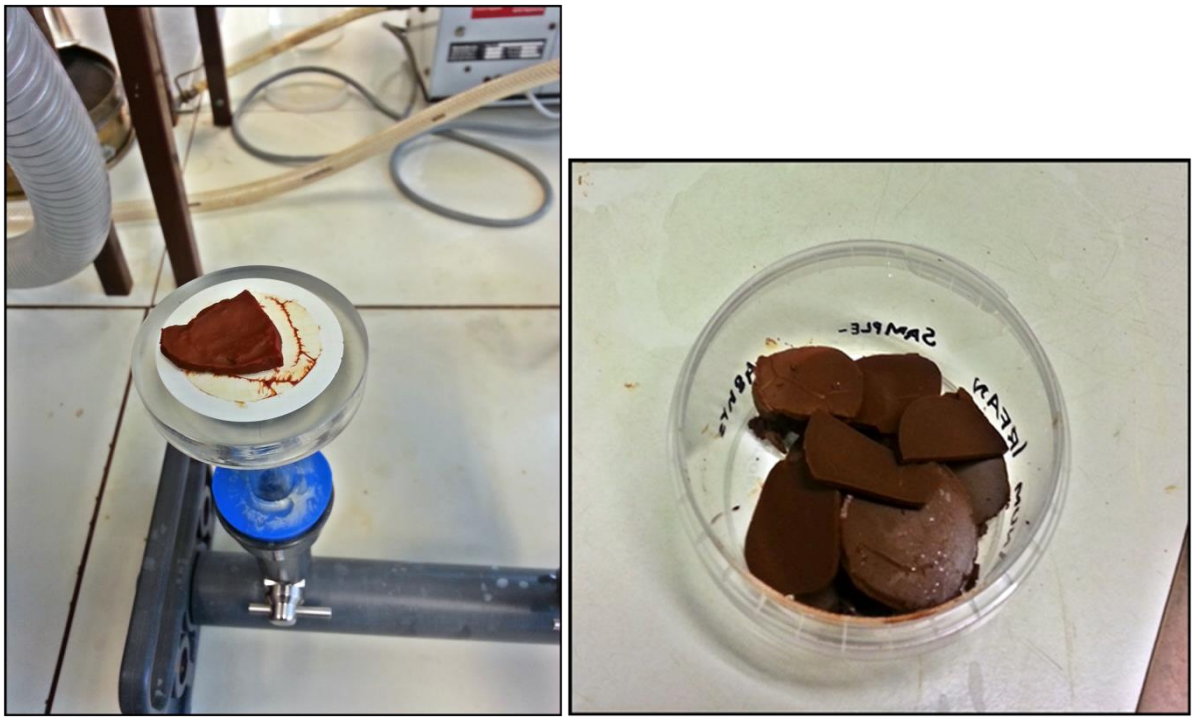

Figure 3-3: The extracted brownish precipitates of pyroaurite after filtration.

3.2. Column experiments (continuous flow)

The column experiments were performed to determine the ability of synthetic pyroaurite for sorption of lead(II) from contaminated water. These experiments were performed twice for evaluation and better understanding of the results. Experiments were conducted under ordinary room temperature. The components of the column experiments are shown in Figure 3-4.

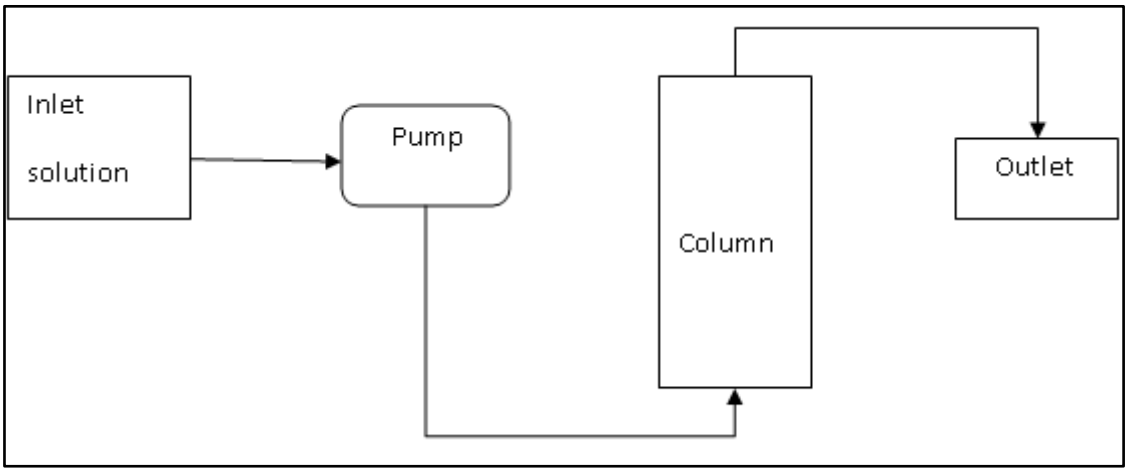

Figure 3-4: Flow chart showing different components used in the column experiment.

First, the inlet solution was prepared by dissolving 10 mg of lead nitrate $Pb(NO_3)_2$ in one litre of distilled (Millipore) water in order to get concentration of 6.3 ppm lead(II) in the solution (see Appendix 1). After shaking the solution well, it was poured into a closed container having a knob and was connected to the ´Gilson's Minipuls 3´ peristaltic pump via tubes. The speed of this pump could be maintained at various flow rates which deliver the smooth and controlled liquid flow without shearing the sample.

Due to limited amount of prepared clay material, it was mixed along with natural sand in order to fill the 10 ml cylindrical column tube and also to improve the flow properties of the packed column. Mineral composition of the sand was determined first via X-ray diffraction technique. The amount of pyroaurite-like material and sand taken was 40 and 60 percent respectively. Both materials were mixed thoroughly and were filled inside the column tube. At the bottom and top of the column, the inside material (clay) was capped by quartz wool to avoid elution of small-grained clay and sand particles along with aqueous solution. One end of the column was sealed with rubber cork and the pipes were adjusted accordingly. Inlet of

the column was connected to the pump and the outlet pipe was put inside small bottles to collect samples as shown in Figure 3-5.

To make the column free from air, it was first fully saturated with distilled water to avoid air bubbles inside the column. The peristaltic pump was adjusted at the speed of 0.10 which gave a flow rate of about 1.25 ml elute per hour. The flow of $Pb(NO_3)_2$ aqueous solution through the column was very slow. Effluent from the column was collected in individual trace metal free bottles at interval of 20 minutes. Experimental setup of clay and sand column is shown in Figure 3-5. It was then calculated how much solution goes into the column and how much effluent is coming out of the column.

Column parameters	**Parameter values**
Height of column	6 cm
Volume of column	9.2 ml
Porosity of the material	0.35 v/v
Average flow velocity	1.25 ml/h
Residence time	2.5 hour
One pore volume	3.24 ml

Table 3-1: Showing parameters used in the experiments for the column tube along with pore volume and average flow velocity.

3.2.1. Sampling method

The first column experiment was kept running for over a period of eight days and 29 samples were collected during this duration. The first 200 minutes were considered to be critical, so ten samples were collected each at interval of 20 minutes giving around 0.8 ml of elute per bottle. These outlet samples were only analysed for detection of lead(II) concentration. While other samples were taken at different intervals in order to get large amount of effluent for other laboratory analysis. The second experiment was conducted for 22 days and about 45 liquid samples were collected for analysis. At the beginning of the experiment, ten outlet samples were collected each at interval of 30 minutes. The column experiments were conducted for a total duration of 30 days. The collected outlet samples during this duration were taken to analyse:

1. The concentration of lead(II), iron and magnesium in ICP-MS.

2. The detection of major anions in the samples using Ion chromatography system.
3. To measure pH of the effluent samples.

Before analysis in ICP-MS, 1% nitric acid (HNO_3) was added in the effluent to avoid precipitation of Fe. The dilution factor was considered for amount of each sample. The inlet aqueous solution of $Pb(NO_3)_2$ was diluted 50 times with 1 wt% HNO_3 whereas the effluent samples were diluted up to 4 to 8 times. The estimated wt% of Pb^{2+} in the solid samples for duplicate column experiments was calculated by using this formula:

$$\Delta Pb^{2+} = C_{Pb^{2+}(solution)} \cdot V_{total} \qquad (3\text{-}1)$$

Where ΔPb^{2+} is the estimated lead amount in solid sample after reaction, $C_{Pb^{2+}(solution)}$ is the total concentration of lead(II) which is pumped through the column, and V_{total} is the total volume of water used for each experiment.

To calculate how much of Pb^{2+}goes into the column ($\Delta n_{Pb^{2+}}$) and how much concentration of lead comes out of the system, the following formula was used:

$$\Delta n_{Pb^{2+}(sample)} = \Delta C_{Pb^{2+}(solution)} \cdot V_{total} \qquad (3\text{-}2)$$

Where ΔC is the change in concentration of lead from inlet and outlet, and V_{total} is the total volume of water that ran through the column.

$$V = Q.t \qquad (3\text{-}3)$$

Where Q is the flow rate per hour, and t is the total time (number of days for running column experiment).

After executing the experiment, the solid material inside the column was also analysed to observe any significant changes in the pyroaurite material after its reaction with heavy metal contaminated water. In order to do so, the column material was divided into four equal portions. One end of the column was cut with a hacksaw, and a plunger which fits inside the cylindrical column was inserted from the other end. By moving the plunger, the inside material was poured out into four different plastic containers. These four samples were washed a little with distilled water and dried in oven at 60ºC for about an hour. These dried samples were then crushed by hand using agate mortar and were examined individually under scanning electron microscope and X-ray diffraction technique.

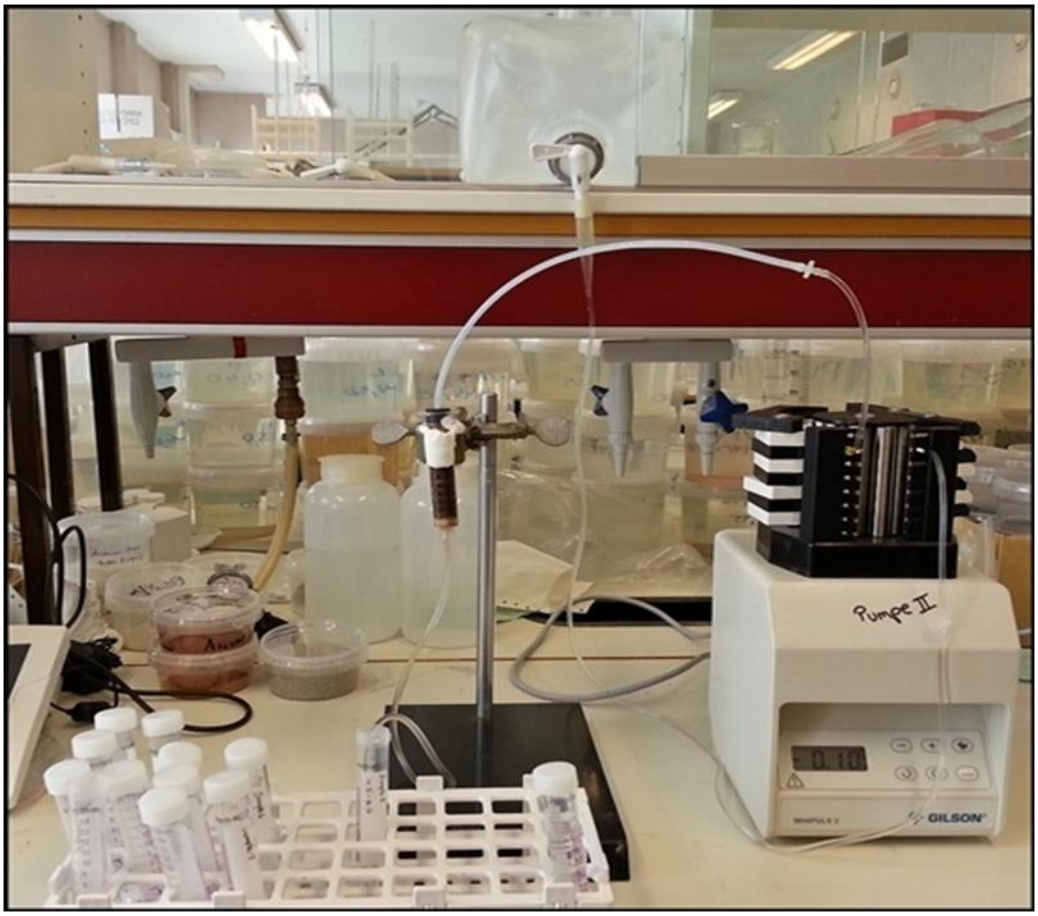

Figure 3-5: The column (continuous flow) experiment set up in the laboratory at room temperature.

4. Analytical methods

For the detailed analysis of the solid samples and for confirmation of elemental composition, different analytical techniques have been used during the work. Analyses of extracted liquid samples have also been done. Analyses have been divided into two parts i.e. solid material analysis and water analysis. List of the methods which have been used are listed below:

Solid material analysis

- Electron microprobe (EMP)
- Scanning electron microscopy (SEM)
- X-ray diffraction technique (XRD)

Water analysis

- Inductive coupled plasma mass spectrometry (ICP-MS)
- Ion chromatography
- pH measurements

The preparation work and analysis of the samples have been carried out at Department of Geosciences, University of Oslo.

4.1. Solid material analysis

4.1.1. Electron microprobe

One thin section of pyroaurite material was prepared for the quantitative micro analysis of the elements present in the material. After preparation of thin section, it was coated with carbon to analyse it under electron microprobe. The thin section was analysed by using electron microprobe Cameca SX100 using the wavelength-dispersive spectrometer (WDS). Elemental mapping for Mg and Fe was done under these analytical conditions:

Accelerating voltage = 15 kV; Beam current: 20 nA (nano Ampere)

X-ray lines used: Fe Kα and Mg Kα

Map parameters: size 1000 * 1000 µm acquired by stage motion, with a step size of 2 µm. Dwell time (per pixel) is 20 ms.

4.1.2. X-ray diffraction analysis

X-ray diffraction is an essential tool for analyses of clay minerals and is used to identify the unknown mineral phases and crystal structure of the sample material. It is also useful for quantitative analysis by determining the amorphous and crystalline components in a mixture.

When a focused beam of X-ray interacts with the sample atoms, part of the beam is absorbed by the sample while some part is transmitted, scattered, refracted and diffracted. When the beam is diffracted, the distance between the planes of the atoms can be measured. The XRD uses X-rays with a known wavelength (λ) to measure the angle (θ) at which the beam is reflected. The spacing (d) between the lattice planes in the crystal is unique for each mineral and can reveal what kind of mineral is being examined. The d-spacing can be calculated using Bragg's Law:

$$n\lambda = 2d \sin\theta \qquad (4\text{-}1)$$

where integer 'n' is the order of the diffracted beam, λ is the wavelength of the incident X-ray beam, 'd' is the distance between adjacent planes of atoms (d-spacing), and θ is the angle of incidence of the X-ray beam (Suryanarayana and Norton, 1998).

4.1.2.1. Sample preparation

To analyse the material in X-ray diffractometer, the prepared material was first crushed into the smaller size particles in an agate mortar by hand. It was then further grinded in the McCrone micronising mill to convert it into powdered form. Grinding was done along with ethanol in the micronizer. Ethanol was used because it vaporises fast. The obtained liquid material was then dried in the electric oven for few hours resulting in fine powder which was used for XRD analysis. The sample powder was then filled in the glass sample holder and was ready to be analysed. A total of nine samples were analysed which includes the original prepared pyroaurite sample and four samples of reacted column material from each column experiment. Samples were analysed for the detection of unknown mineral phases using Bruker D8 advance XRD instrument. The XRD result analysis has been performed using the Diffrac.Eva software.

4.1.3. Scanning electron microscope

Scanning electron microscope was used for detailed imaging and analysis of our samples .In SEM; images of the samples are originated by bombarding the sample with a focused beam of high energy electrons which interacts with the sample atoms and generate signals. These signals are identified by electron detectors and become visible on the computer screen. The signals provide information about the texture and the chemical composition of the sample. Different detection modes can be used in order to get compositional or topographic contrast. Variety of signals which are produced by this microscope includes: Back scattered electrons (BSE), Secondary electron (SE), Cathodoluminescence (CL), Characteristic X-rays. The energy dispersive spectrometer (EDS) is attached to the microscope, which assists in generating characterististic X-rays of the selected area and creates images (Reed, 2005).

Microscope comprises of an electron gun which acts as the electron source, having a negative potential and helps in accelerating the electrons towards the sample. Electron gun along with electron lenses combines to form a column. Function of these electron lenses is to focus the beam on the specimen. This electron beam travels down into the column while the beam diameter is demagnified by the condenser lenses. The beam is focused by the objective lenses to create an intense image of the sample (Reed, 2005).

SEM has the ability to achieve very high resolution micrographs of the sample. Secondary electron images display high resolution topographic contrasts. The contrast in the image is determined by the morphology of the sample. Secondary electrons are low energetic as they are emitted from very close to the sample surface (Reed, 2005).

Back scattered electron images (BSEI) contains compositional information as the heavy elements with high atomic number are scattered strongly than the lighter elements. It exhibits the information about the distribution of the different elements in the sample. However, image resolution is lower than that of the secondary electron images (Reed, 2005).

Energy dispersive spectrometer (EDS) is used for qualitative and semi quantitative determination of the elemental composition in the sample. Qualitative analysis includes the x-ray line identification of elements in the spectrum. Quantitative analysis determines the concentration of elements in the sample by measuring the X-ray line intensities emitted from

the specimen for each element and measuring these intensities with those from the standard samples of known composition (Reed, 2005).

4.1.3.1. Sample preparation

SEM analysis has been executed using JEO2 JSM-6460LV Scanning electron microscope with Link Inca Energy 300 (EDS) under the supervision of Berit Løken Berg. Back scattered electron image (BSEI) and secondary electron image (SEI) have been used in combination to identify the elemental composition and structure of the synthetic material before and after the reaction. For this study, carbon and gold coated stub mounted samples, one carbon coated thin section and few uncoated stub mounted samples have been analysed under scanning electron microscope. The uncoated samples were analysed at low vacuum mode. Two of the samples from prepared material were gold coated. Both of the samples were similar in composition but the only difference was one of them was dried in oven for 24 hours and the other one was dried for 48 hours at 50°C. Four reacted samples were analysed from individual continuous flow experiment.

4.2. Water analysis

The liquid effluent (outlet) samples from the experiment were taken for further analysis by the following mentioned techniques:

4.2.1. pH measurements

Metrohm 702 SM Titrino pH meter was used to measure the pH of the inlet aqueous solution along with the outlet samples (elute) from the column experiments. The system was calibrated by putting the electrode in the solutions of pH 4, 7 and 10 before measuring pH of the samples. This was done at ordinary room temperature i.e. 25°C. pH of the $Pb(NO_3)_2$ aqueous solution along with pH of the outlet samples from continuous flow experiment were measured in the laboratory.

4.2.2. Inductively coupled plasma- mass spectrometry (ICP-MS)

Inductively coupled plasma- mass spectrometry is a modern day analytical technique for trace elements detection, having numerous applications in the fields of biomedical sciences, geo-chemistry, and geology. It is a powerful tool for high precision analysis of trace elements

with considerable applications in earth sciences. The trace metal detection limit ranges from high (parts per million) ppm to low (sub parts per trillion). Mass spectrometry utilizes the elemental mass in order to perform qualitative and quantitative analysis. Usually the sample should be in liquid form in order to analyse it in ICP-MS. However, solid samples can also be analysed by hitting the solid sample by a laser beam and converted into dust sized particle (Longerich et al., 1990; Thomas, 2013).

Liquid samples have been analysed for determination of lead (Pb), using quadrupole mass analyser system ICP-MS, bruker Aurora M90 (Q-ICP-MS) at Department of Geosciences, University of Oslo. The detection limit for lead (Pb) in this instrument ranges from 0.01 ppb (minimum) to 1 ppm (maximum) (person. communication).

First, the liquid sample is pumped into the nebulizer through a peristaltic pump normally at the speed of 1 ml/minute. The peristaltic pump helps in the constant flow of liquid. In the nebulizer, the liquid is converted into the fine aerosol droplets by the flow of argon gas, which is then sorted out from larger molecules in the spray chamber. From the spray chamber, only small droplets entered into the plasma by means of a sample injector. In the plasma torch, positively charged ions are generated which afterwards travelled to the mass spectrometer which is also known as the mass separation device. Mass spectrometer is even capable of separating elements having same atomic number but different atomic mass units. Here ions are separated according to their mass to charge ratio and are send towards the ion detector where ions are converted into the electrical signal (Thomas, 2013).

4.2.2.1. Sample preparation

Samples collected from both column experiments were analysed in ICP-MS to determine concentrations of lead, iron and magnesium. In order to analyse the liquid samples, the amount of sample is also taken into consideration. Amount of sample required to analyse in ICP-MS varies according to the sample introduction system. On average about 10 ml of liquid sample is required. The volume of the sample needed to make around 10 ml solution depends upon the element which is needed to be determined (Longerich et al., 1990).

Before analyzing the samples in ICP-MS, the solutions were diluted with 1% nitric acid (HNO_3). The inlet aqueous solution of $Pb(NO_3)_2$ was diluted 50 times with 1% HNO_3, because the concentration of lead in the solution was 6.3 ppm. Whereas, the effluent samples

were diluted up to four to eight times to increase the amount of sample for analyses. The concentrations of iron and magnesium in the effluent were also monitored using ICP-MS. 18 samples were analysed for the detection of magnesium in ICP-MS. The eluted samples were diluted up to 200 times with 1% HNO_3 in order to analyse magnesium.

4.2.3. Ion chromatography

It is a liquid chromatographic method for the analysis and separation of both organic and inorganic cations and anions. Components of a typical ion chromatography system have been shown in Figure 4-1.

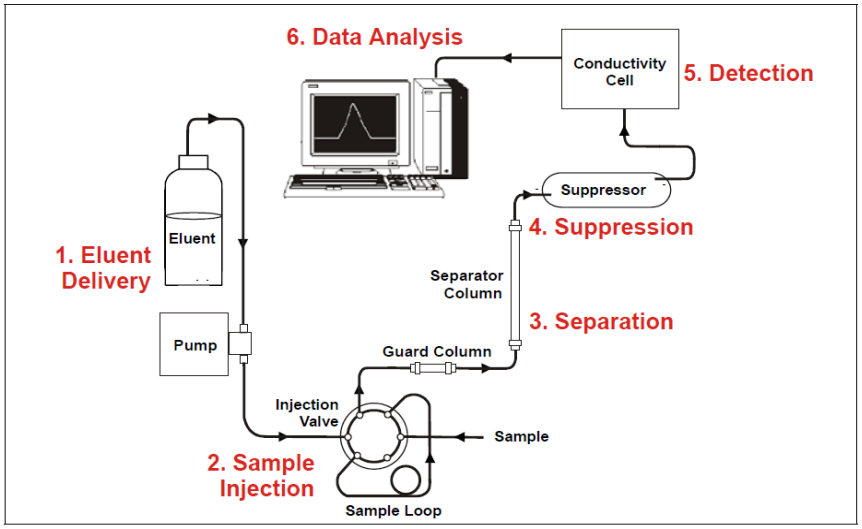

Figure 4-1: Workflow for ion analyses after Corporation (2006).

A high pressure pump is used to pump the liquid eluent into the stationary phase (column). The eluent used in our case is potassium hydroxide (KOH). This stationary phase comprises of small polymer resins; commonly known as ion exchange resins. These resins can be either anion exchange or cation exchange resins having positive and negative charged sites respectively. They have ability to attract the oppositely charged ions, in this way required ions gets separated. In cation exchange chromatography, positively charged molecules are attracted towards a negatively charged solid support. The case is opposite in anion exchange chromatography where negatively charged molecules show affinity to a positively charged solid support. The sample is introduced into the path of flowing eluent via sample injector which is present just before the column. The eluted sample is detected by means of a detector (usually conductivity detector) which can be used with or without suppressor system. The purpose of the suppressor is to convert sample ions in conductive form by reducing the

background conductivity of electrolytes present in the eluent. The signals are displayed as chromatogram on the computer screen using chromatography software. The system calibration was first done with known standards and the samples were injected later. The obtained data of the samples is then compared with that of the known standards (Seiler et al., 1994; Weiss, 2008).

The Dionex ICS-2000 Ion chromatography system was used for measuring major anions in our collected samples from column experiment. Concentration of nitrate was analysed for inlet lead(II) nitrate solution along with the collected effluent samples from column experiments. Samples from both experimental runs were analysed.

5. Results

The synthesized pyroaurite was first analysed to determine its structure along with chemical and elemental composition. However, the reacted material inside the column was also analysed after running the column experiments. The results obtained from several analytical techniques used in this study are divided into following three sections:

1) Pre-experimental characterization of the synthesized pyroaurite.
2) Column experiments (liquid sample analysis).
3) Post-experiment analyses of the reaction products.

5.1. Pre-experimental characterization of the synthesized pyroaurite

5.1.1. X-ray diffraction (XRD)

The material was first analysed using XRD to determine crystal structure and to investigate which mineral phases have been formed. Figure 5-1 displays the XRD diffractogram of prepared pyroaurite material before reaction. The primary and secondary minerals formed during preparation have been identified. The results confirm the presence of a pyroaurite-like material in the sample along with noticeable amounts of brucite $Mg(OH)_2$. In addition, chloromagnesite ($MgCl_2$) is also a prominent mineral in the sample. Brucite was present in abundance. Although presence of quartz was not expected but was also present in traces. The formation of unexpected mineral phases might be due to the presence of impurities in the salts which were used in the preparation of pyroaurite mineral (Figure 5-1).

The XRD analysis of the prepared sample shows that synthetic pyroaurite was highly amorphous and show lack of well-developed crystal phases. The peaks in the diffractogram come out to be very broad and on a rough estimation, it can be said that the material is approximately 30-35% crystalline.

Figure 5-2 illustrates the minerals present in the sand which were used as a column material along with pyroaurite. The sand composition was analysed before running the experiment. The sand was mostly composed of quartz with minor amounts of feldspars i.e. albite ($NaAlSi_3O_8$) and microcline ($KAlSi_3O_8$).

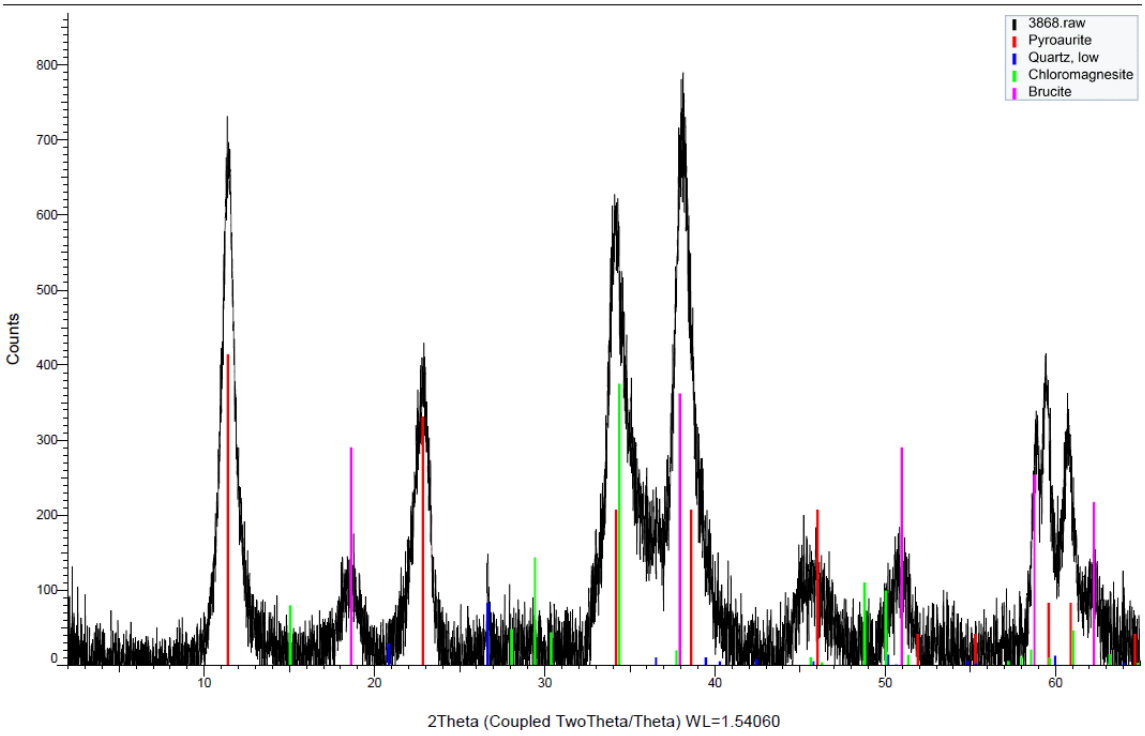

Figure 5-1: X-ray diffractogram showing different minerals present in the prepared clay sample. Presence of pyroaurite has been confirmed but consdiderable amount of brucite is also present along with some chloromagnesite.

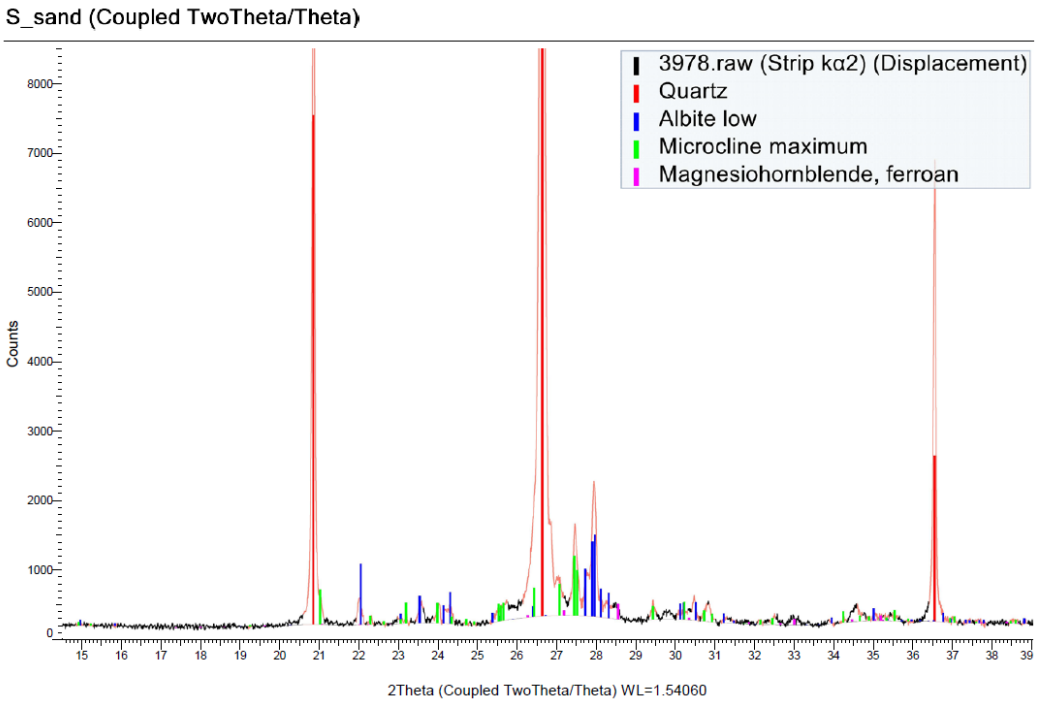

Figure 5-2: X-ray diffractogram representing the primary and secondary minerals present in the sand used in the column experiments.

5.1.2. Electron microprobe

The thin section of synthetic pyroaurite was first observed under optical microscope. Figure 5-3 shows a representative part of a thin section. This part was analysed with the electron micro-probe to determine the amount of magnesium and iron present in the sample. The result in Figure 5-4 shows that the sample is rather homogeneous. Magnesium and iron are present throughout the sample. Hence, it becomes challenging to differentiate between the locations of two elements.

Figure 5-3: Image of pyroaurite thin section from optical microscope.

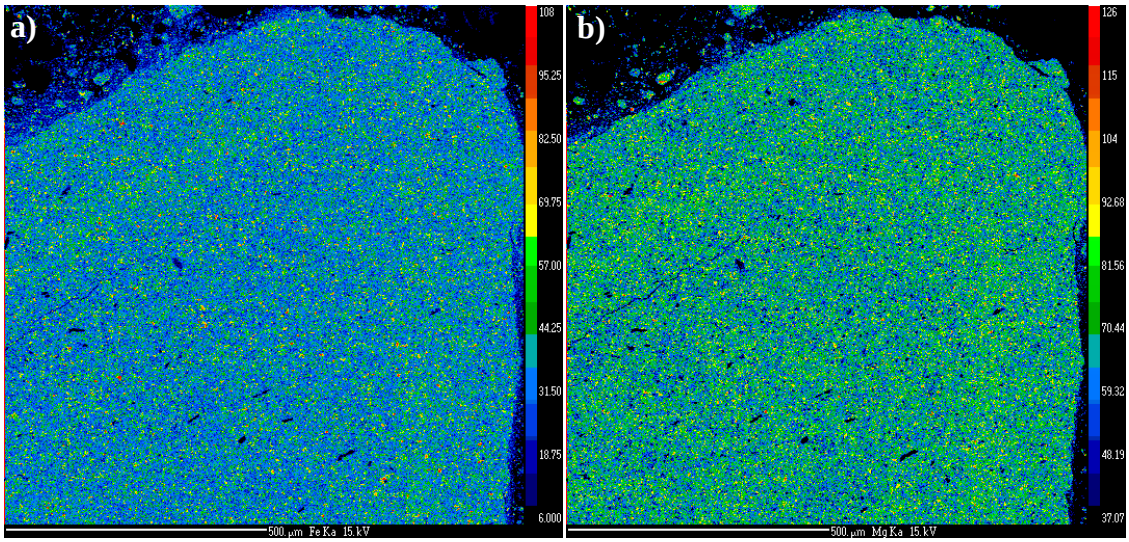

Figure 5-4: a) Element map of iron. b) Magnesium from thin section of synthetic pyroaurite using electron microprobe. The scale on the right side demonstrates the intensities of element from high (red) to low (dark blue).

In the element maps it can be seen that around the dark ring area, magnesium is present in slightly higher amounts than iron (Figure 5-4a, b). It could be possible that more particles from pyroaurite material are present in that area giving strong signals but there is a probability that magnesium is present in higher quantities as compared to iron. The higher quantity of magnesium in the synthetic material has also been confirmed using other analytical techniques.

5.1.3. Scanning electron microscope

SEM micrographs and EDS analysis using SEM were carried out to determine the sample structure and composition. Topographic images of the synthetic mineral using SEM are displayed in Figure 5-5: The synthetic material was analysed under scanning electron microscope to observe its crystal structure and morphology in detail, and also to determine chemical composition and element mapping. Two gold coated samples were observed, one of the sample was dried in oven for 24 hours while the other sample was kept in oven for 48 hours to improve the crystallinity of the material. The structure of synthesized material showed that it was not crystalline (Figure 5-5). However, a few crystals have been observed at higher magnifications. Mostly the crystals were not grown completely. On the other hand, lot of particles or fragments have been formed. It seems that they are having some kind of tiny overgrowths on them as seen in Figure 5-5.

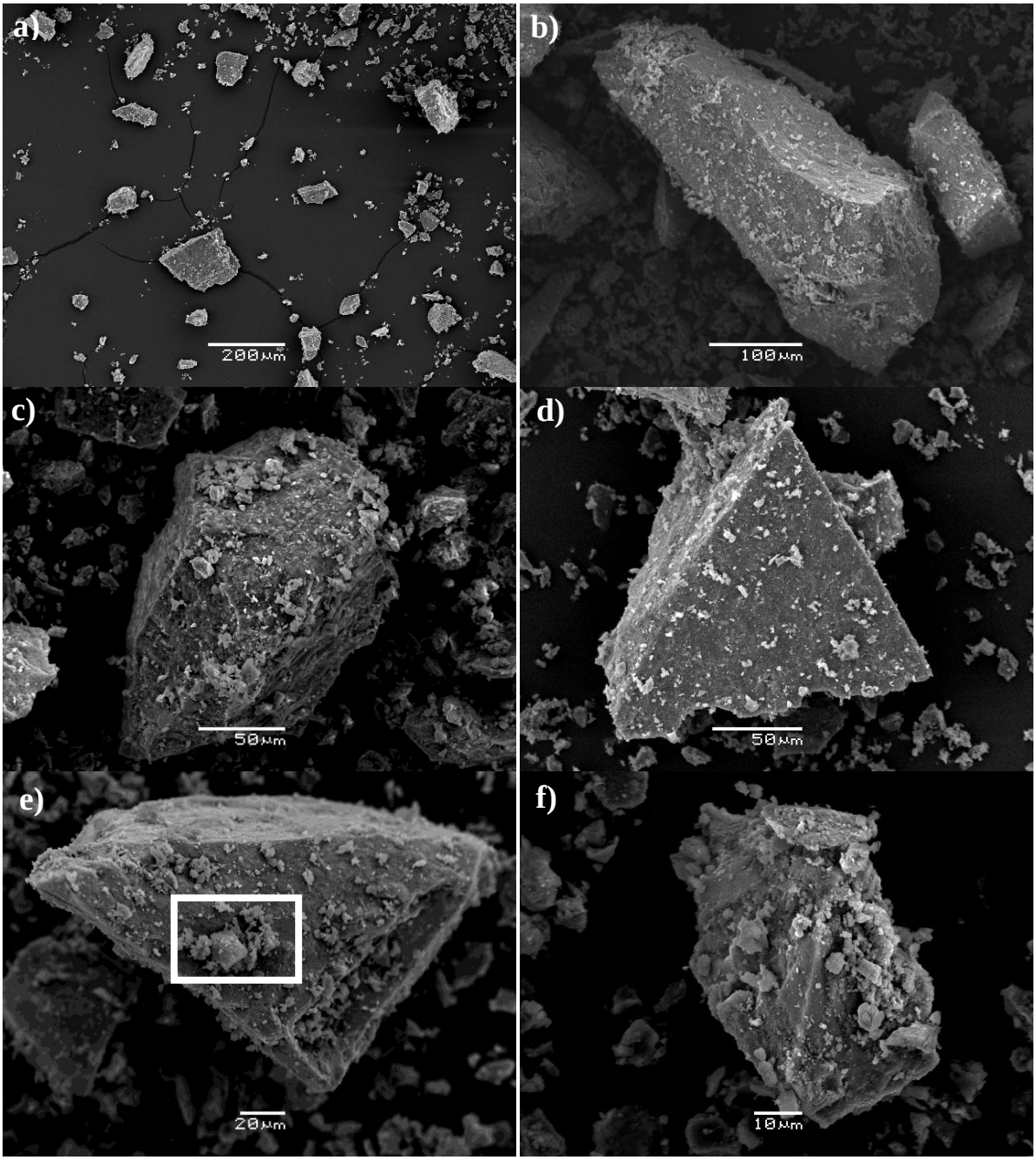

Figure 5-5a-d: Showing secondary electron images of gold coated synthetic pyroaurite mineral samples from SEM taken at different magnifications representing the structure of the mineral formed. e, f) Showing particles and fragments of pyroaurite formed synthetically. Large particles have some overgrowths on them.

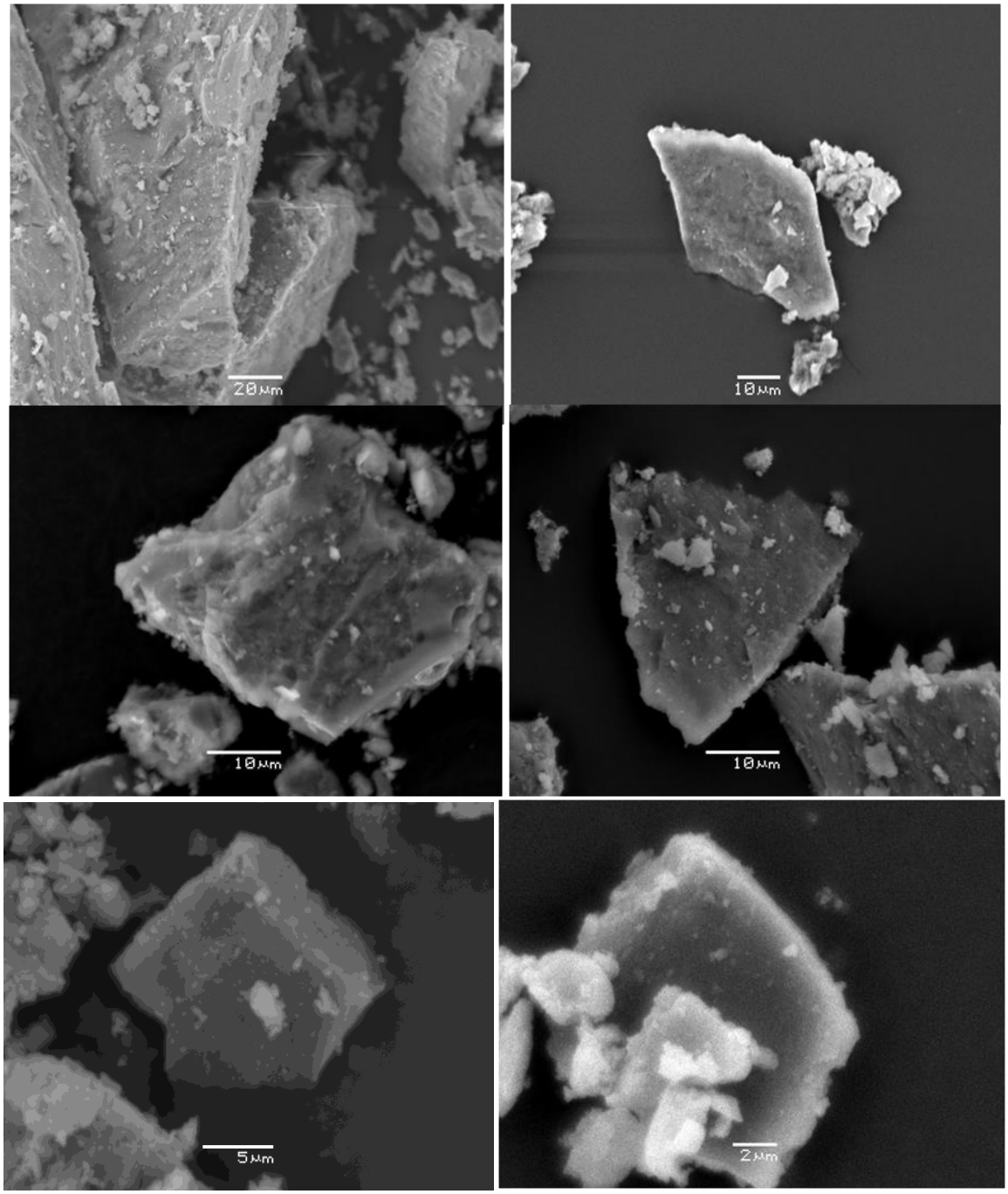

Figure 5-6: SEM micrographs of gold coated pyroaurite samples showing structures of specific grains at different magnifications.

Quantitative analysis of the material was also done to determine the ratio of magnesium and iron and other elements present in the sample. Through EDS spectra and imaging from SEM, it seems that the synthesized material was a homogenous mixture and has uniform distribution of Fe and Mg which were added in the form of salts. Carbon along with oxygen was also found in the samples confirming the presence of carbonate. There was some carbon

contribution from the carbon tape as well on which the samples were mounted on the stub. Sample also contains some impurities which may be introduced from the chloride salts utilized for preparing the compound.

The 24 hour dried sample was observed under microscope first, but very small amounts crystals were observed, so the rest of the material was kept again in oven for another day. The purpose was to improve the crystallinity of the material. But results from both the samples were similar. None of the samples showed considerable amounts of crystals.

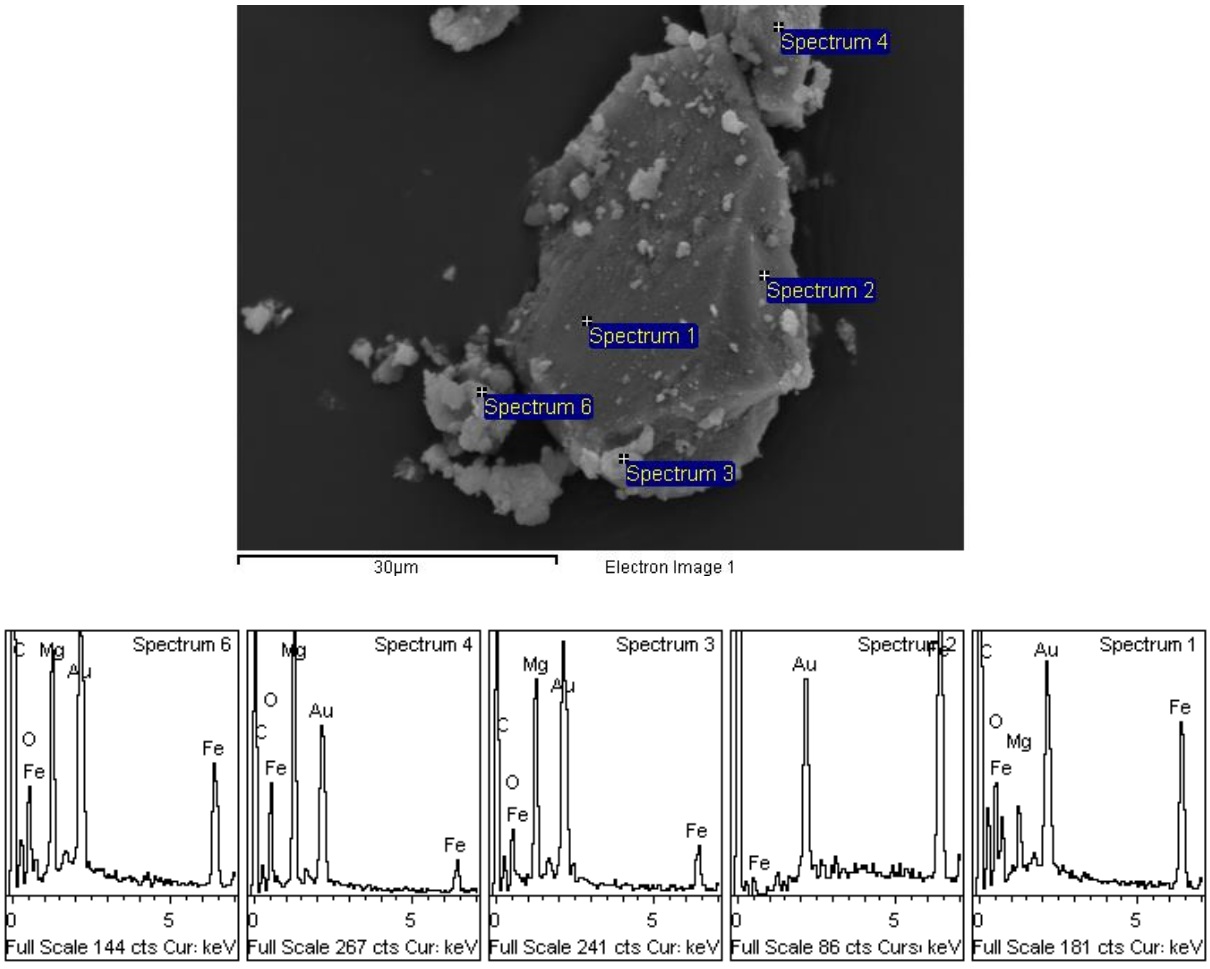

Figure 5-7: BSE image along with EDS spectra of the selected areas representing presence of Mg, Fe, O and carbon. Gold peak is due to gold coating of the sample.

Table 5-1 displays the quantification of various elements found in Figure 5-7. Magnesium and iron are present in different quantities. These results reveal that the sample material is not truly homogeneous. In some regions higher amount of Fe is found whereas in some areas Mg is higher than Fe. For instance, in the region of spectrum 2, Fe is present in excessive amounts than Mg but in other regions Mg quantities are higher than the Fe ones. There are

chances that iron oxides have been formed in the regions where there is excess of Fe as compared to Mg. The source of higher amounts of carbon is most probably contributed from carbon tape on which the sample was placed.

Spectrum	**C**	**O**	**Mg**	**Fe**
Spectrum 1	51.82	28.42	3.42	16.34
Spectrum 2	28.12	6.35	2.27	63.26
Spectrum 3	47.92	27.79	16.31	7.97
Spectrum 4	36.40	40.25	18.83	4.52
Spectrum 5	38.33	38.65	16.51	6.51
Spectrum 6	44.43	29.31	12.29	13.97
Mean	41.17	28.46	11.60	18.76
Std. deviation	8.61	12.11	7.11	22.26
Max.	51.82	40.25	18.83	63.26
Min.	28.12	6.35	2.27	4.52

Table 5-1: Quantification of various elements found in the selected area of the sample (Figure 5-7). All the results are in atomic wt%.

Table 5-2 displays presence of different elements of selected areas from Figure 5-8. High carbon content is present along with considerable amounts of Mg and Fe. In areas of spectrum 2 and 3, magnesium is present in excess as compared to iron. However, in regions of spectrum 4 and 5, almost equal quantities of iron and magnesium are present.

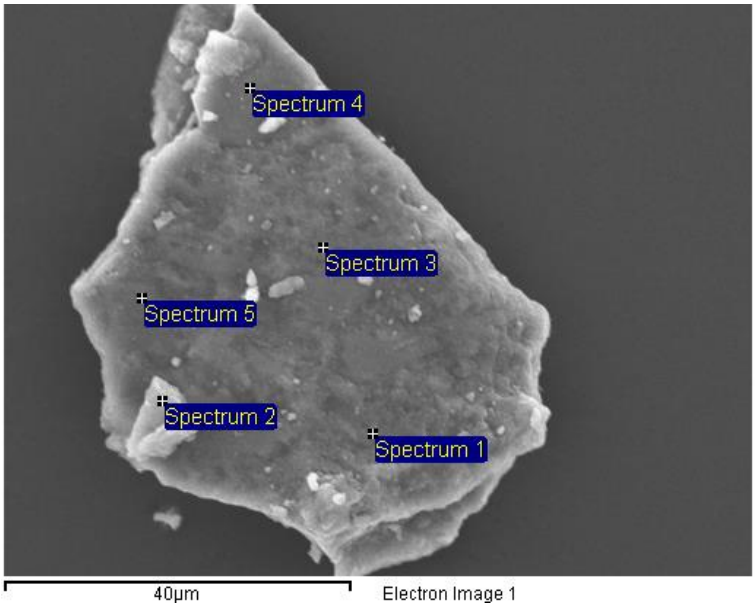

Figure 5-8: BSE image representing a selected grain for quantification of elements.

Spectrum	**C**	**O**	**Mg**	**Fe**
Spectrum 1	29.42	36.28	20.61	13.70
Spectrum 2	36.10	40.99	17.01	5.90
Spectrum 3	36.40	36.48	17.99	9.13
Spectrum 4	23.00	36.65	19.84	20.51
Spectrum 5	28.72	35.20	18.47	20.61
Mean	30.73	37.12	18.18	13.97
Std. deviation	5.62	2.24	2.09	6.63
Max.	36.40	40.99	20.61	20.61
Min.	23.00	35.20	15.47	5.90

Table 5-2: Elemental quantification in atomic wt% of the selected grain in Figure above.

Another selected particle from synthesized material is shown in Figure 5-9 along with EDS spectra for different location showing high peaks for magnesium. The selected areas were then analysed quantitatively (Table 5-3). The mean value for Mg is considerably higher than that of the Fe.

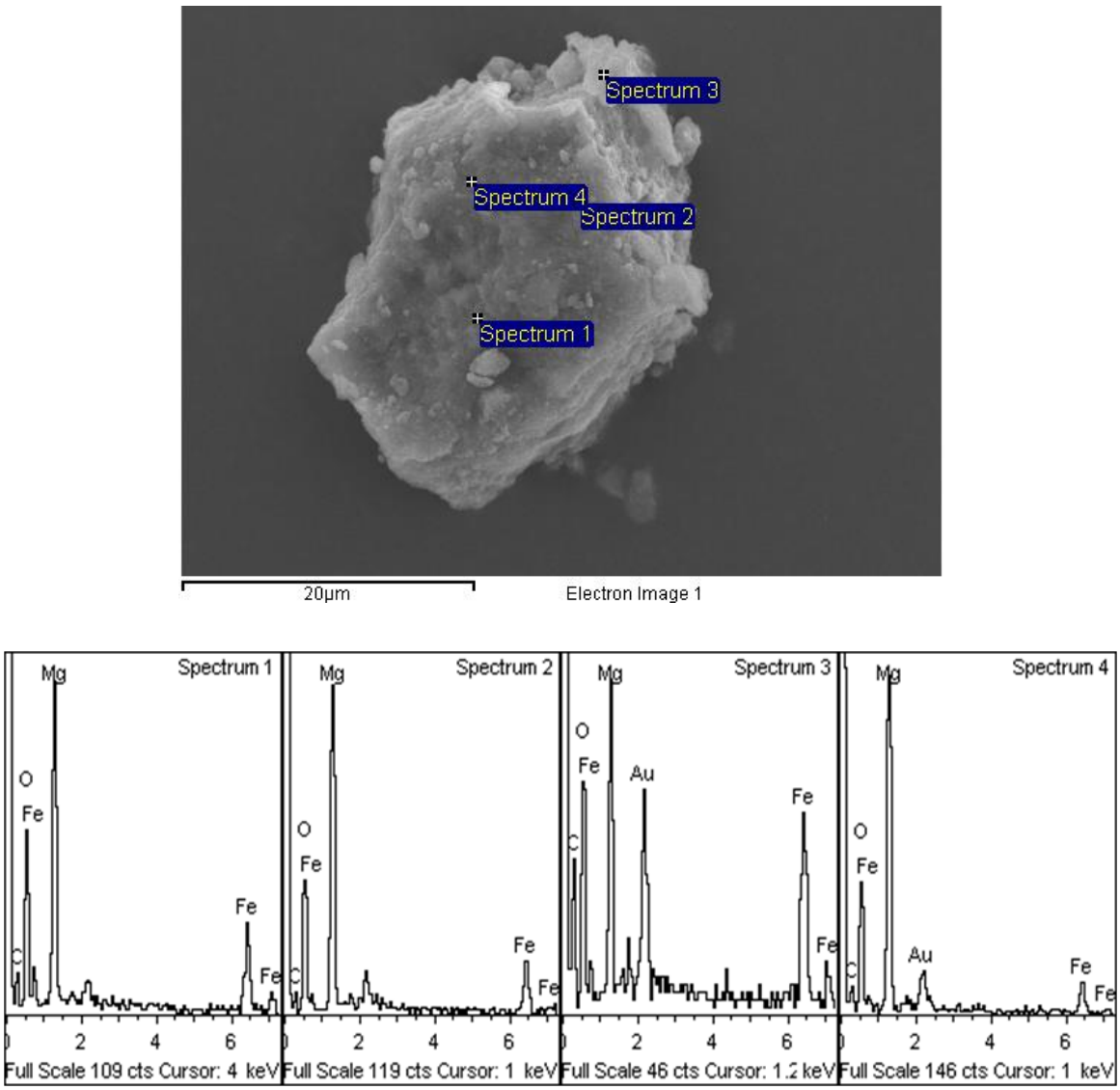

Figure 5-9: BSE image along EDS spectra showing selected areas of fragment for analysis.

Spectrum	**C**	**O**	**Mg**	**Fe**	**Total**
Spectrum 1	19.79	33.52	20.87	13..82	100
Spectrum 2	18.47	35.75	26.62	19.16	100
Spectrum 3	31.69	26.48	9.84	20.99	100
Spectrum 4	21.40	37.02	27.24	10.34	100
Mean	22.84	33.19	21.14	16.17	100

Table 5-3: Elemental quantification for Figure 5-9 b. in wt%.

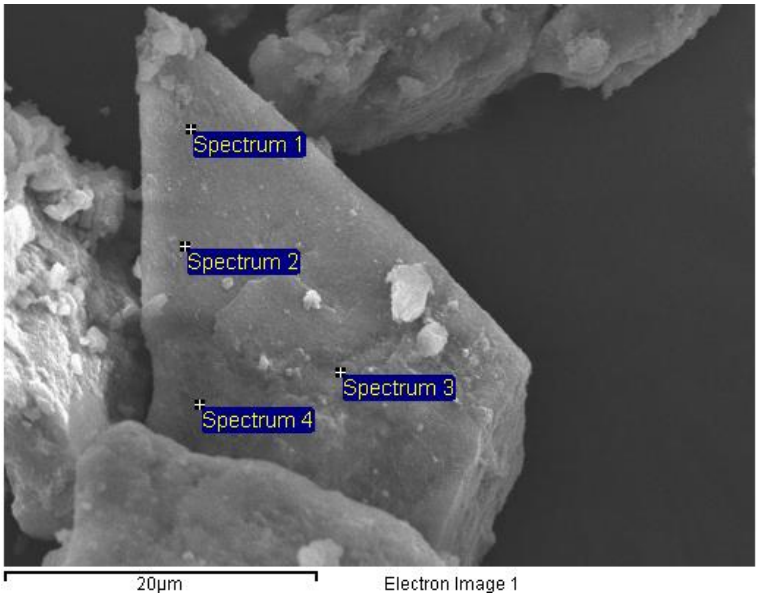

Figure 5-10: Shows the chosen area from stub-mounted sample of pyroaurite used to analyse chemical composition.

The chemical formula for pyroaurite ($Mg_6Fe_2(CO_3^{2-})(OH)_{16}.4H_2O$) reveals that it has 6 atoms of Mg, 2 atoms of Fe and one atom of C. In this way quantity for Mg should be higher than Fe which is somehow true in our case as seen in Table 5-2, Table 5-3, and Table 5-4. However some abnormalities have also been observed where Fe quantities are higher than Mg ones as displayed in Table 5-1.

Spectrum	**C**	**O**	**Mg**	**Fe**
Spectrum 1	25.62	38.20	23.42	12.75
Spectrum 2	11.81	39.91	23.40	24.89
Spectrum 3	16.80	47.40	29.07	6.73
Spectrum 4	18.14	44.03	27.23	10.60
Mean	18.09	42.38	25.78	13.74
Std. deviation	5.71	4.14	2.84	7.84
Max.	25.62	47.40	29.07	24.89
Min.	11.81	38.20	23.40	6.73

Table 5-4: Elemental composition from selected areas from Figure 5-10.in atomic %. Magnesium is present in higher amounts than Fe in the selected specific area.

Thin section studies of the samples were also carried out for further analyses. Figure 5-11 displays the elemental maps for detected elements in the sample. On the whole it is evident

that Fe and Mg are present homogeneously in the sample. But the quantification of selected areas in (Table 5-5) reveals that in some specific areas of particles higher amounts of Fe are present while in some parts low Fe and high Mg amounts are present.

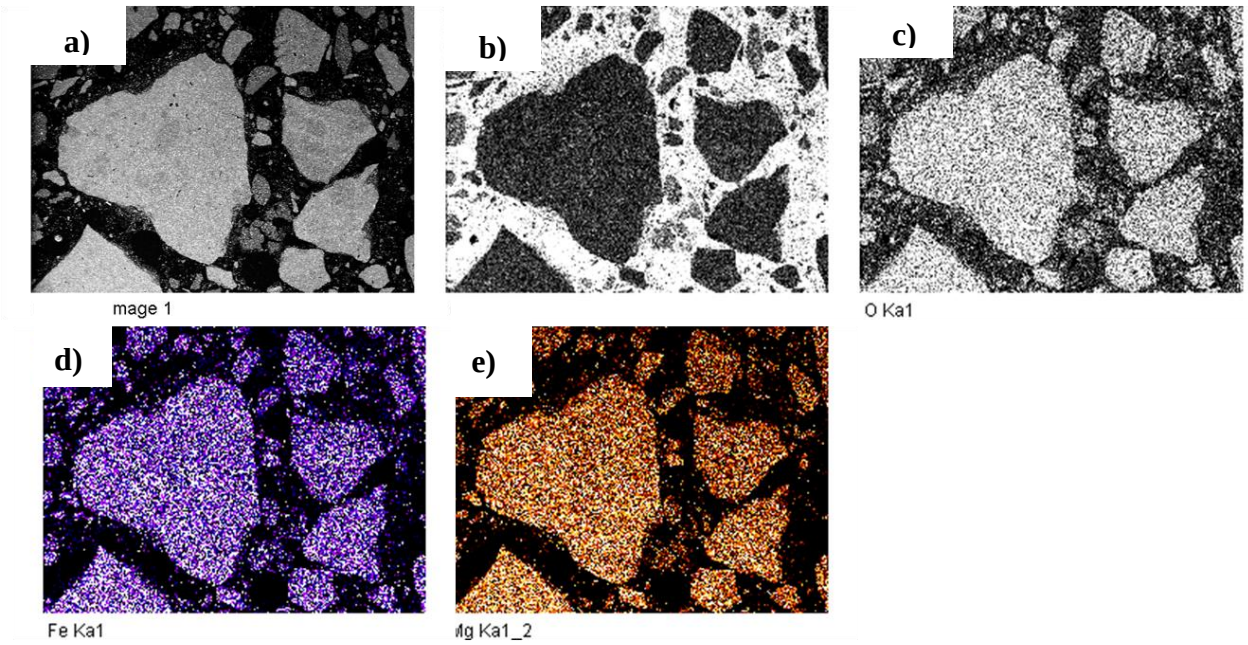

Figure 5-11: a) Shows the element map of selected region from thin section b) Map for carbon c) Map for oxygen d) Map for iron, and e) Map for magnesium. The white areas represent the elements at their highest intensities.

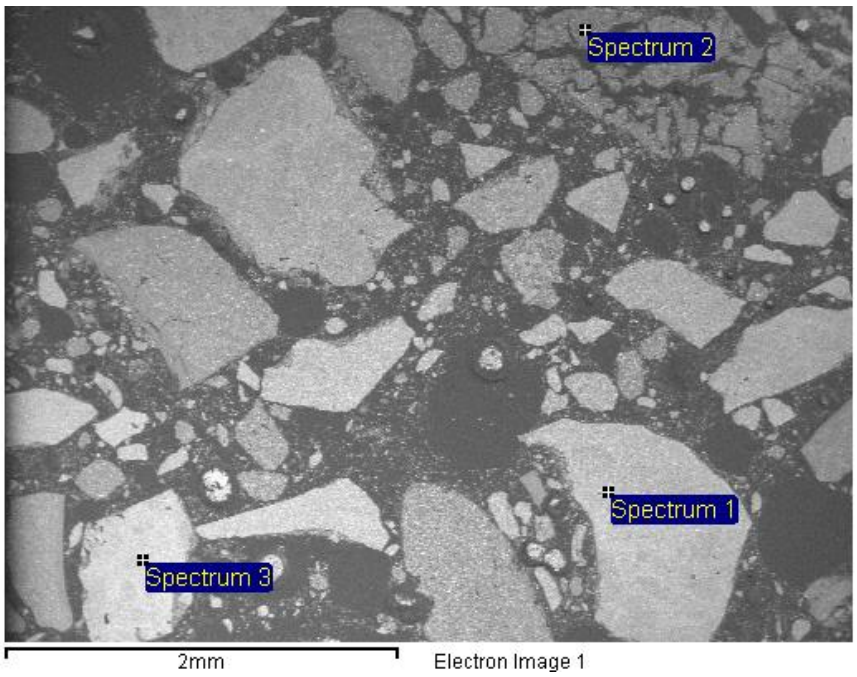

Figure 5-12: Selected area from thin section for quantification analyses of elements.

Spectrum	O	Mg	Fe	Total
Spectrum 1	21.52	32.50	29.98	100
Spectrum 2	22.06	32.34	25.59	100
Spectrum 3	25.02	35.75	30.22	100
Mean	22.87	33.53	28.59	100

Table 5-5: Elemental quantification for thin section in wt%.

Elemental mapping was also carried out along with SEM in order to analyse the presence of different elements in the sample. Figure 5-13 depicts the location for two minerals Fe and Mg in the chosen area of the sample.

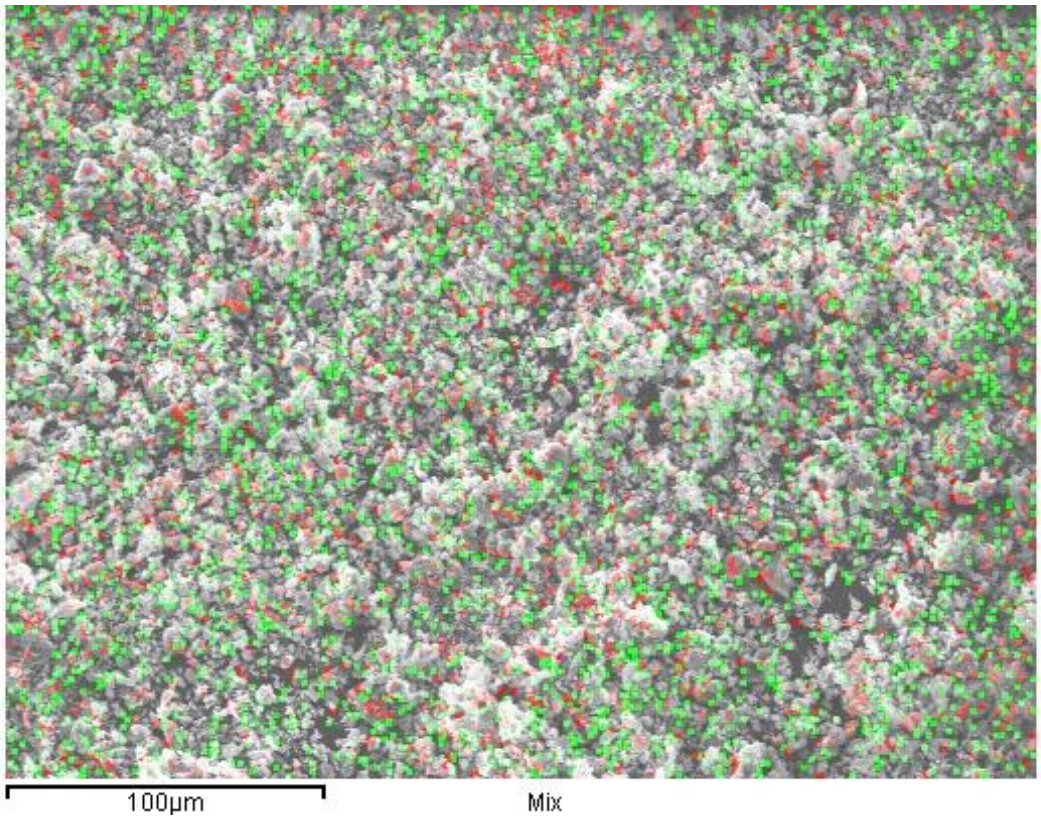

Figure 5-13: Elemental map of the selected area of pyroaurite sample for locating Fe and Mg. Map also indicates the presence of both elements at different locations with red dots representing Mg while green dots represent the presence of Fe in the area.

5.2. Column experiments

The column experiments were repeated twice. The aqueous outlet samples were analysed to determine their pH and to detect major anions and their concentrations in the samples.

5.2.1. pH measurements

pH of the prepared inlet $Pb(NO_3)_2$ solution and effluent samples for run one and two of the experiment are shown in Figure 5-14 and Figure 5-15 respectively. The measured pH of aqueous $Pb(NO_3)_2$ solution was around 6.5, though pH for this solution was not much stable. Hence, it can be said that the solution was slightly acidic.

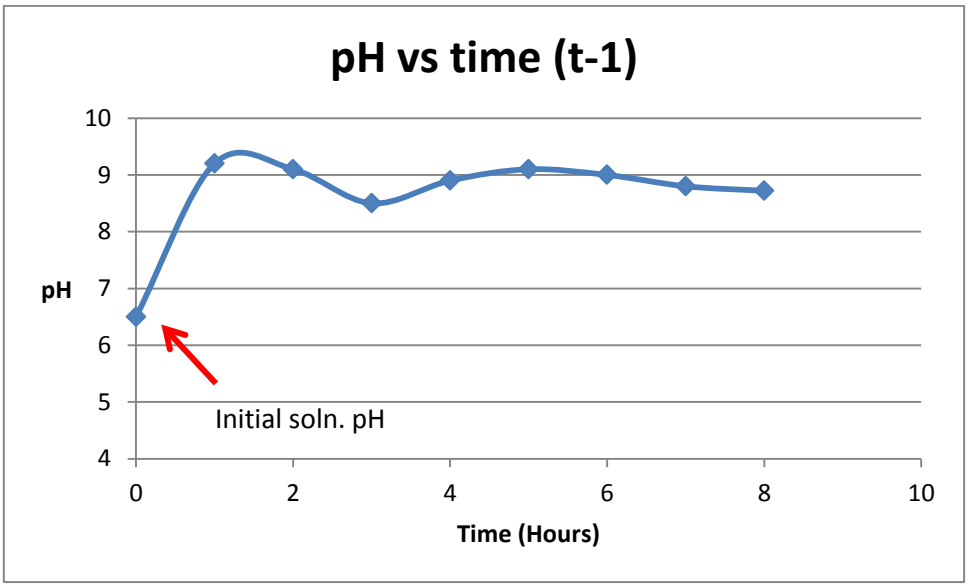

Figure 5-14: Comparison of pH of the inlet and outlet samples from first column experiment which is plotted against number of hours. The arrow indicates pH of the incoming lead(II) nitrate solution whereas the other points show pH of the outlet samples.

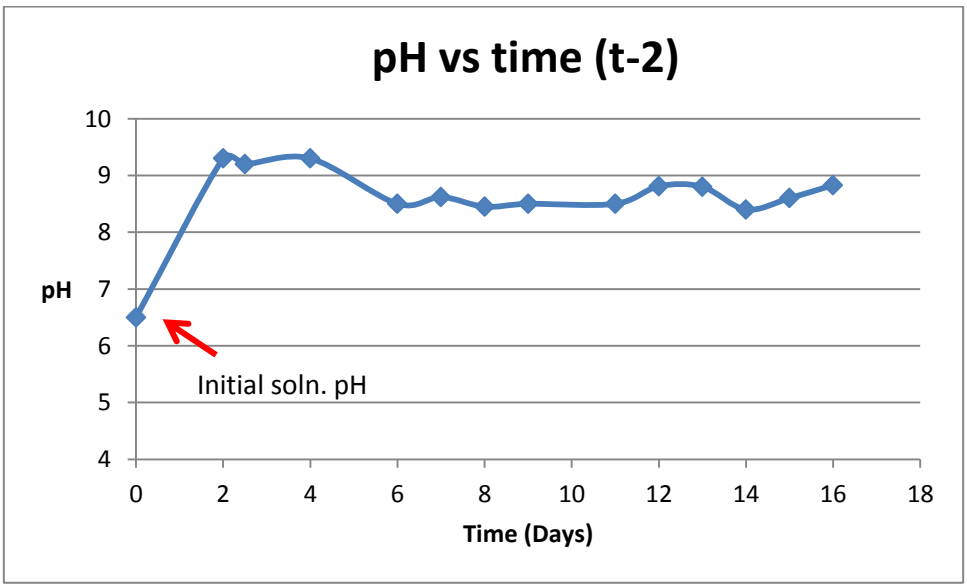

Figure 5-15: pH of the outlet samples from second column experiment. pH is plotted against number of days when samples were taken. The arrow indicates 6.5 pH of the incoming lead(II) nitrate solution.

On the other hand, pH for the outlet samples was observed between 8.5-9.3. This showed that all of the samples were basic. None of the outlet sample was acidic or neutral. Although, a linear decreasing or increasing trend in the plotted graphs have not been observed. The tabulated results of measured pH for all samples are shown in appendix 2 (Table A and B).

5.2.2. Ion chromatography

The amount of nitrate in the eluted samples from both experiments was analysed with respect to the initial aqueous solution of lead(II) nitrate. Figure 5-16 represents the concentration of nitrate from first column experiment. The graph shows a decreasing trend in nitrate concentration with time. Initial concentration of nitrate in the inlet solution was compared with the number of days along with the nitrate concentration in the eluted samples.

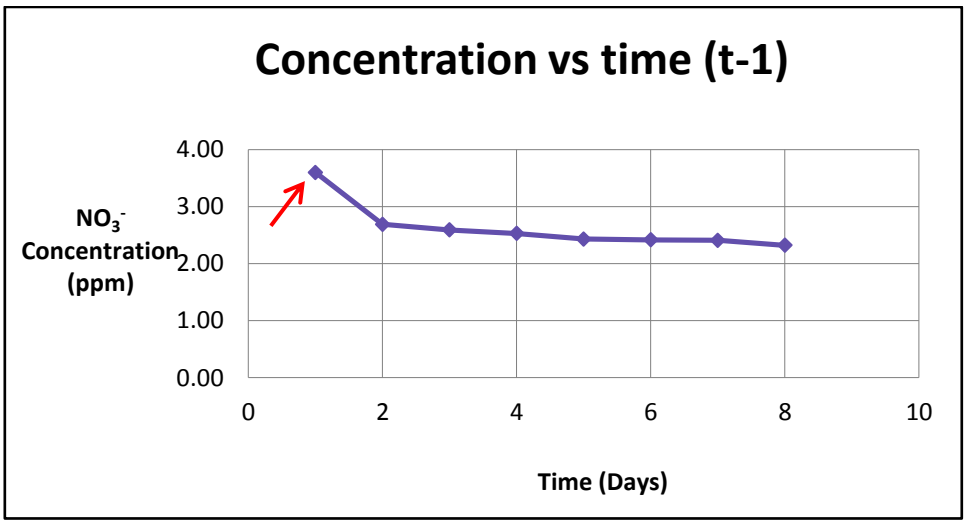

Figure 5-16: Graph showing a decreasing trend in nitrate concentrations in outlet samples with the passage of time from first column experiment. The arrow represents the nitrate concentration (3.6 ppm) of the incoming $Pb(NO_3)_2$ solution.

Figure 5-17 and Figure 5-18 represent results from second experiment. Five samples were collected in one day each after 2 hour while running the experiment. After that one sample was taken in each day. The concentration of nitrate ions in incoming solution is 3.60 ppm whereas, the outlet concentration ranges from 2.69 to 2.33 ppm. The detailed collected data for major anions from trial one and two of the experiments can be seen in appendix 2 (Table C and D.)

A downward shift in NO_3^- concentration with increasing time can be seen in these graphs. There could be a possibility that the nitrate anions are sorbed inside the column. These anions

showed affinity towards synthetic pyroaurite material. This result supports the evidence as in reality, pyroaurite has anion exchange behaviour.

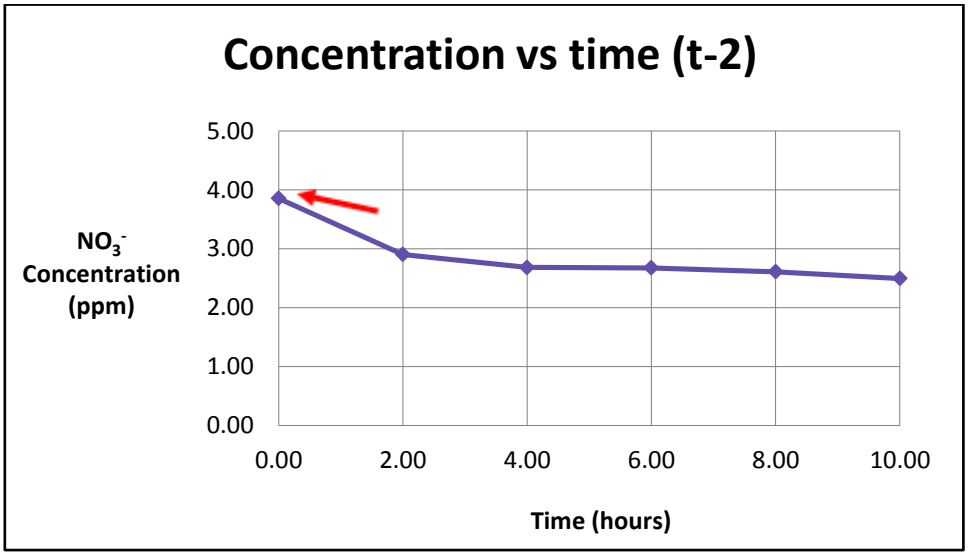

Figure 5-17: Graph representing the results of nitrate concentrations in outlet samples taken in one day from second experiment. The arrow represents the concentration of nitrate (3.6 ppm) from the incoming $Pb(NO_3)_2$ solution.

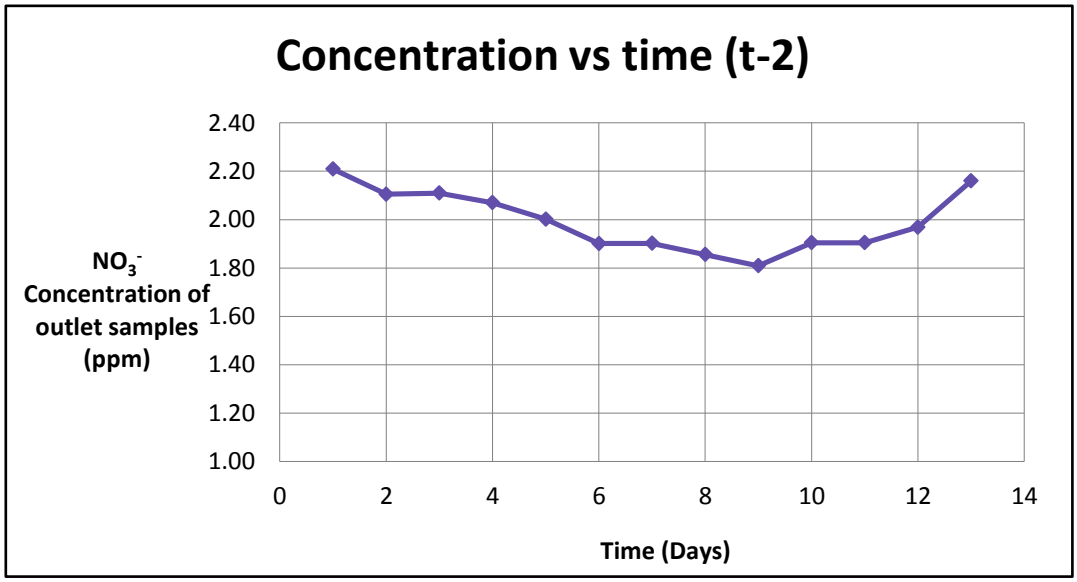

Figure 5-18: Showing nitrate concentration in effluent samples taken at different days from second trial.

5.2.3. ICP-MS

Concentration of lead in inlet and outlet solutions was analysed in ICP-MS. The initial concentration of lead(II) in inlet solution was 5850 ppb. Figure 5-19 illustrates the concentration of lead in outlet samples plotted against number of pore volumes from the first

column experiment. Each sample was taken after 20 minutes interval. Total concentration of lead in the samples from first flow through experiment comes out to be 26.07 ppb. However, in this figure at certain points, drastic increase in lead concentration can be observed. This sudden rise in concentration can be possibly caused by small fragment or particle that may has eluted by chance through the column into the outlet sample and may has dissolved there. The results can be seen in appendix 2 (Table E).

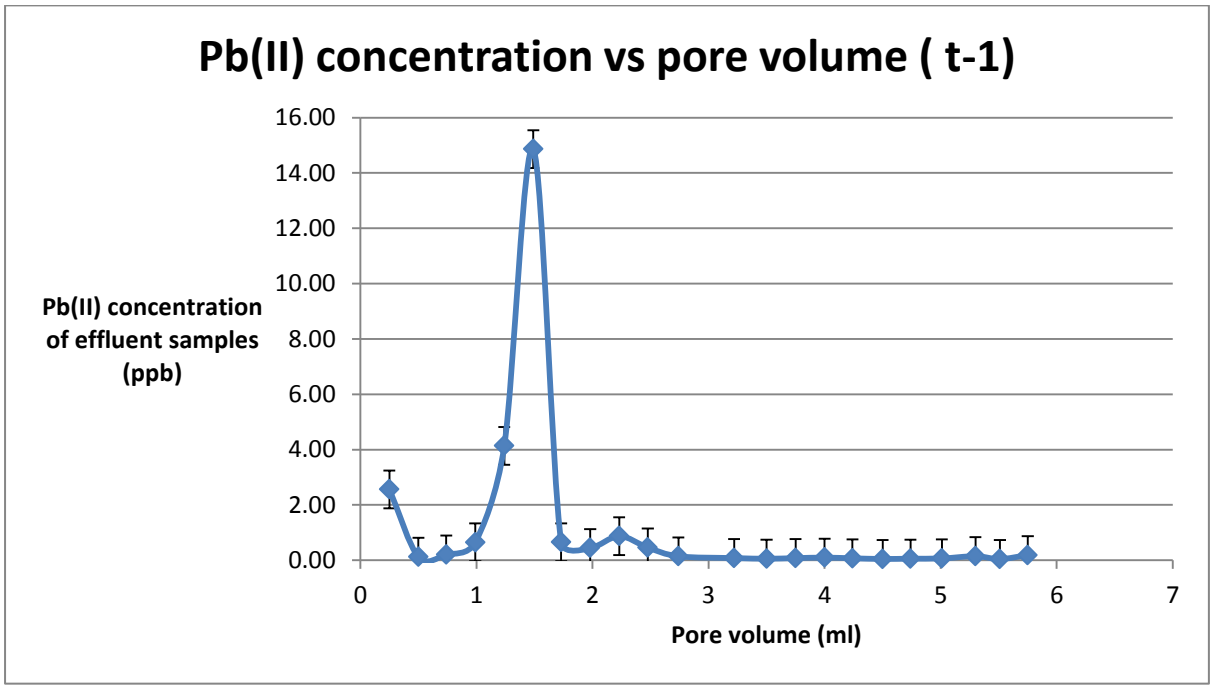

Figure 5-19: Results from first continuous flow experiment. Concentration of lead in outlet samples is plotted against number of pore volumes. The uncertainty from measurement is shown as error bars.

The concentration of Pb(II) found in second column experiment is shown in Figure 5-20. It can be seen clearly that Pb(II) concentration in samples is dropping down and very low amount of lead(II) is coming out in the effluent samples. Although, incoming Pb^{2+} concentration is considerably higher as compared to what is coming out. The total concentration of Pb^{2+} in the effluent samples from second column is 4.2 ppb. Samples were collected for about 3 weeks and data of samples from each day has been gathered and plotted for second run. It can be noticed that concentration falls down even more from 0.1 ppb till 0.02 ppb. The results can be seen in appendix 2 (Table F).

On the basis of the results from ICP-MS, it has been confirmed that around 5849 ppb of Pb(II) is going into the column and in 30 days of experiment duration, around 30.3. ppb Pb(II) is detected in the effluent. The Pb(II) concentration in the outlet samples is very low

revealing that the rest of Pb(II) is sorbed inside the column or it is also possible that secondary mineral growth has started. Hence, it is evident that lead(II) has shown affinity to the pyroaurite-like compound. So, further evaluations have been carried out in order to confirm this suspicion.

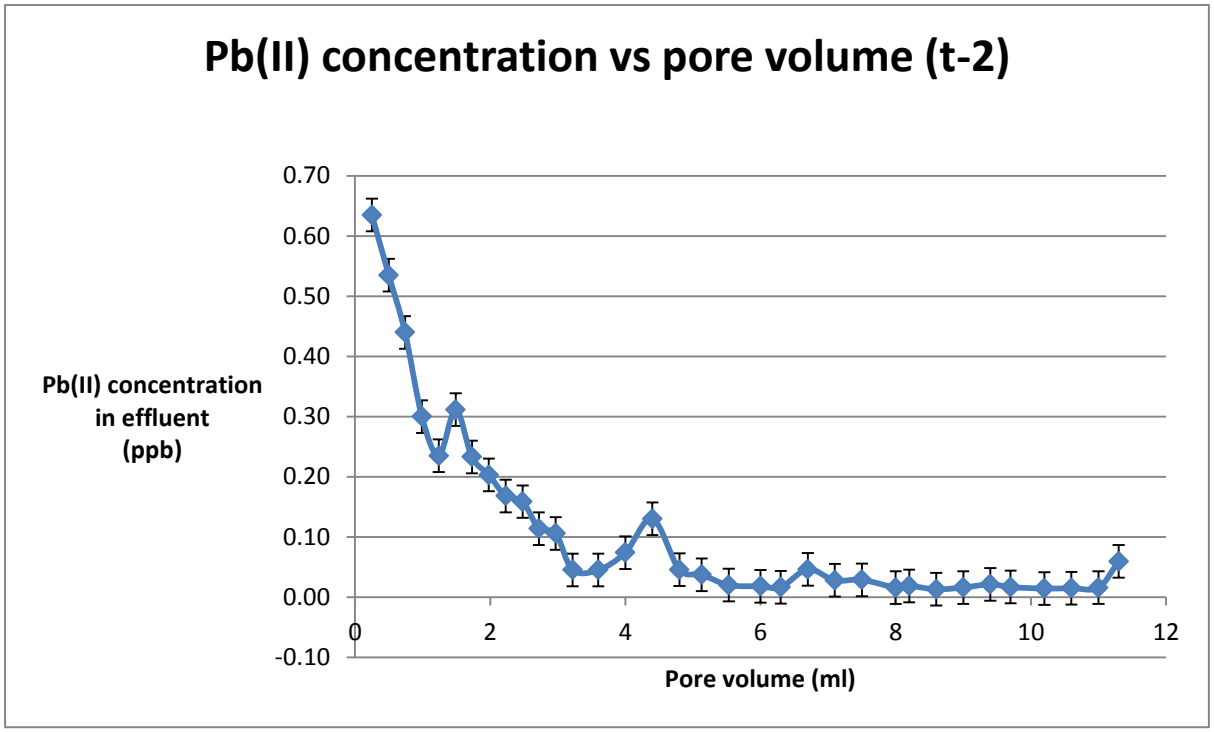

Figure 5-20: Results of second column from all the samples. Concentration of lead plotted against number of pore volumes. The samples were taken at 30 minutes interval. The uncertainty from measurement is shown as error bars.

The estimated percentage of Pb^{2+} in 10 grams of column material i.e. sand and pyroaurite for first and second column is 0.014% and 0.039% respectively using equation 3.1. Calculations can be seen in Appendix 1 b.

The following equation (3.2) has been used to calculate how many grams of Pb^{2+} remains inside the column after the experiment.

$$\Delta n_{Pb^{2+}(sample)} = \Delta C_{Pb^{2+}}.V$$

Volume of water (V) = 900 ml

$$\Delta C_{Pb^{2+}} = C_{inlet} - C_{outlet}$$

$$\Delta C_{Pb^{2+}} = 5.849 \text{ ppm}_{inlet} - 0.030 \text{ ppm}_{outlet}$$

$$\Delta C_{Pb^{2+}} = 5.819 \text{ ppm} = 0.00581 \text{ g/L}$$

Now: $\Delta n_{Pb^{2+}(sample)} = 0.0058 * 0.9 = 0.00523$ gram

So it is calculated that 0.00581 grams of $Pb^{2+}$was present in the inlet solution and the total concentration of lead in the effluent is just 0.00003 grams while the rest of the lead (0.00523 grams) might have remained inside the column. In terms of percentage, almost 99% of Pb^{2+} has been taken up by the synthetic pyroaurite which means that the material has potential to remove dilute lead(II) from water. The value of ΔC (change in concentration of Pb^{2+}) is 0.00581 while the total mass of incoming Pb^{2+} was 0.00584. This result reveals that 99.5% of Pb^{2+} is taken up by the pyroaurite column material. The results from both the graphs in Figure 5-19 and Figure 5-20 show that concentration of Pb^{2+} in the effluent is well below the drinking water standard i.e.10 ppb as suggested by World Health Organization.

Furthermore, to get insight into the process, the reacted column material was analysed by means of XRD and SEM. In ICP-MS, concentration of magnesium and iron has also been analysed. Concentration of iron (Fe) was analysed in few samples but it comes out to be very low. None of the samples showed noticeable amounts of Fe. That is why results for Fe are not included here. On the other hand, in case of magnesium (Mg), high concentrations have been found.

In the inlet solution of $Pb(NO_3)_2$ per litre distilled water, the concentration of Mg was negative. While running the column experiment, the aqueous solution gets passed from the column material and the magnesium which was present in our sample gets in contact with the solution running through. The results for Mg concentration in the outlet samples are plotted against time (Figure 5-21). The concentration seems to decrease with passing time. However at a certain point, the concentration again rises (see Appendix 2 (Table G)).

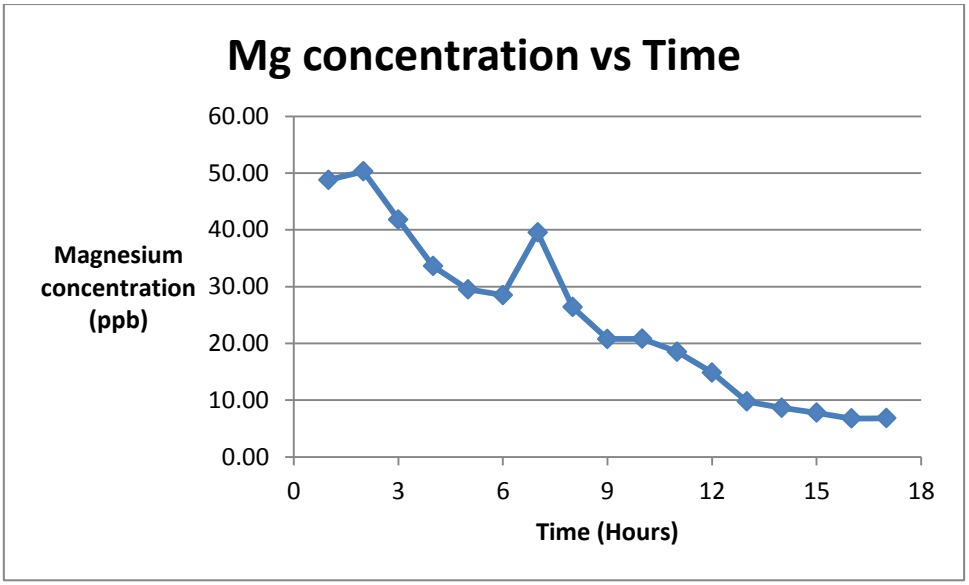

Figure 5-21: Concentration of magnesium (ppb) analysed in ICP-MS.

5.3. Post-experimental analyses of the reacted solids

5.3.1. Characterization of solid column material using XRD

After running the column experiments, the reacted column material was analysed using XRD to determine what changes have occurred in the material and to investigate if new mineral phases have been formed after eluting the material with lead(II) nitrate solution. The results from both experiments have been presented in this section. The reacted material from column was divided into four sections (Figure 5-22). Each of these samples were analysed separately and were compared with each other to observe the differences.

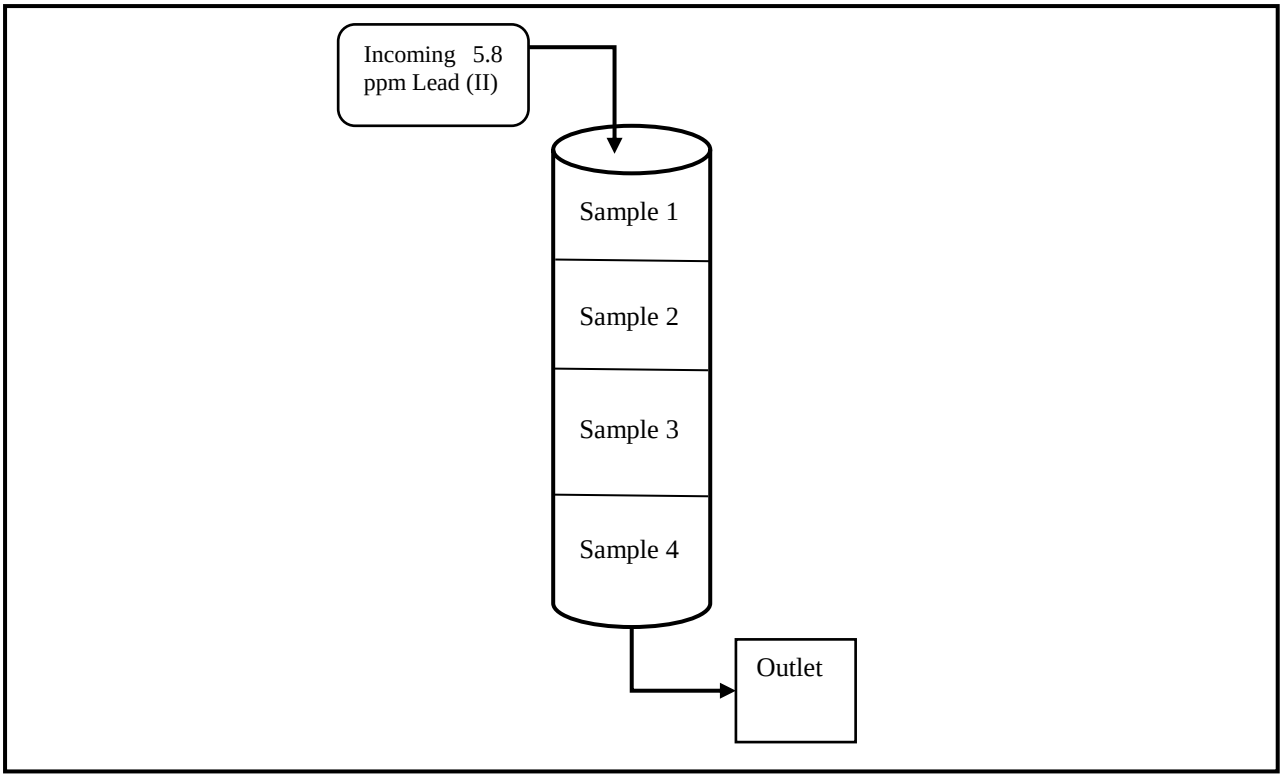

Figure 5-22: Division of reacted solid column material into four samples for analyzing using SEM and XRD.

Figure 5-23 represents the after-effect of the first column experiment from section one. In Figure 5-24 , the results from each four section are compared with each other and composition of all the samples was similar.

Figure 5-25 and Figure 5-26 illustrate the results from second column experiment. The results were found similar to first experiment. None of the sample showed any modification or alteration after reaction of material with solution of $Pb(NO_3)_2$. It was anticipated that after the reaction new phases on pyroaurite can be formed but initiation of new phases have not been detected.

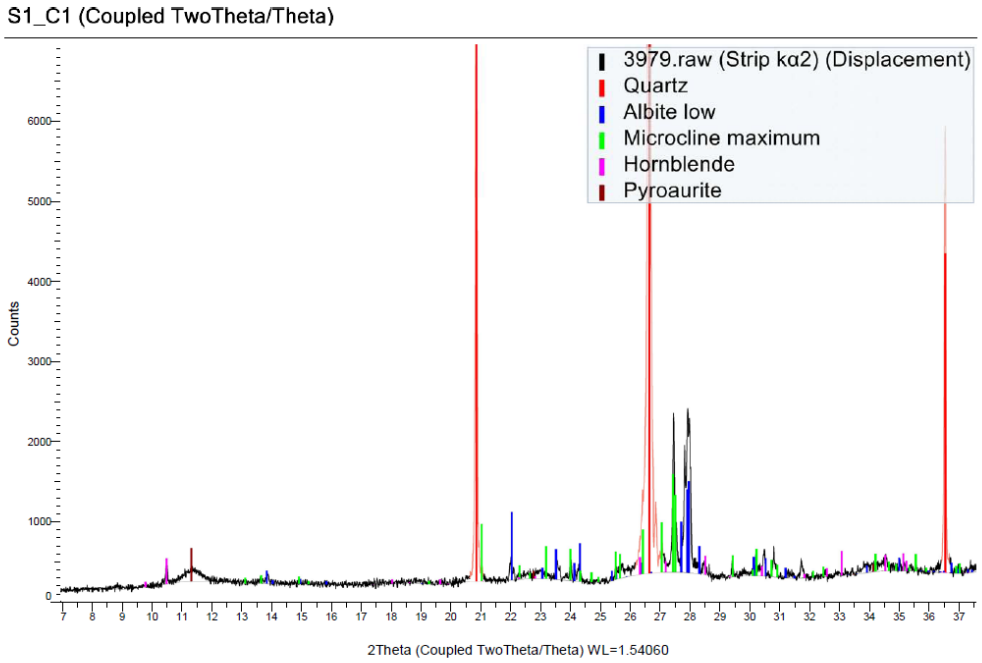

Figure 5-23: XRD pattern displaying results from first column experiment.

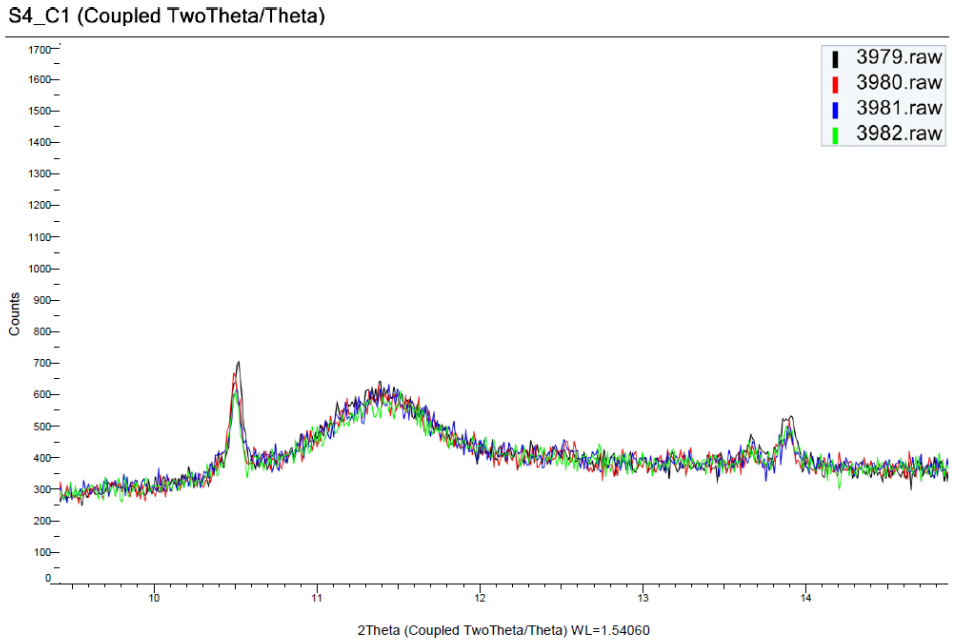

Figure 5-24: XRD pattern from all the four sections of the reacted column material lying on top of each other for comparison.

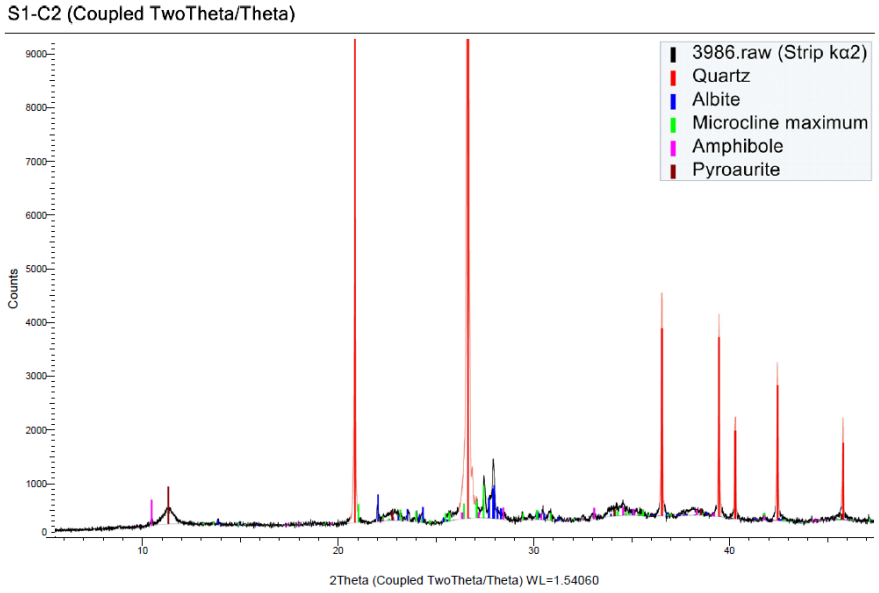

Figure 5-25: XRD pattern from sample 1 of second column experiment representing different minerals present in the reacted sample.

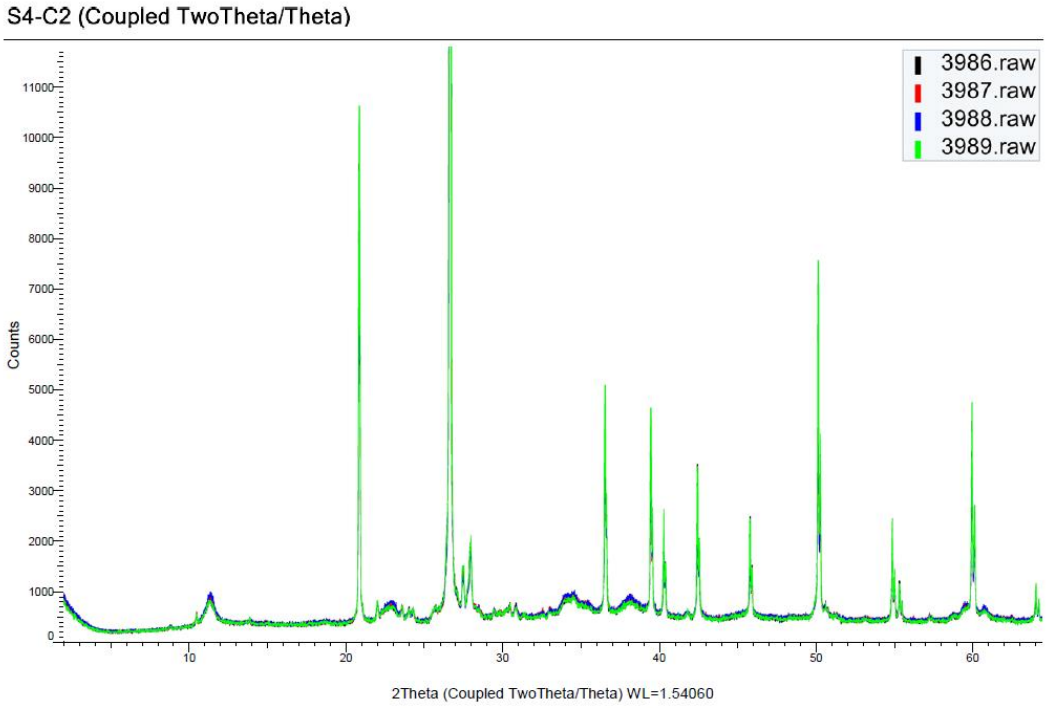

Figure 5-26: XRD pattern results from all the four sections of reacted material representing no alteration in second experiment.

The results shows that apparently lead(II) did not form any new phase. However, it is possible that a new phase might have been developed but the quantity was too low to be detected by this technique.

5.3.2. Characterization of solid column material using SEM

Four samples from each column experiment were analysed under scanning electron microscope to study the changes in composition, morphology and to observe if any new phases are formed on pyroaurite material in the column after its reaction with lead(II) nitrate solution. The basic purpose was to investigate if lead is adsorbed or if it has affinity to the synthetic pyroaurite mineral. The uncoated samples were observed as back scattered electron images at low vacuum. Only one out of four samples from first experiment showed presence of lead(II). Sample 1 which is located near to the inlet solution displays traces of lead(II) (Figure 5-22).

From the second column experiment, the results were almost similar as of first experiment. The upper two samples (sample 1 and 2) showed the presence of lead while the lower two samples near outlet did not show any signs of lead(II) in them. Heavy metal lead(II) having atomic number 82, appears as a brighter element in back scattered electron images (BSEI). So, it becomes convenient to mark the presence of lead in the samples as it appears as a brighter white part while scanning. Figure 5-28 shows some areas of the samples in which presence of lead(II) has been confirmed.

In the uncoated samples it was difficult to get EDS spectra of certain areas of interest because the grains were loosely attached to the stubs. When the beam falls on the specific area of our interest, grains disappears due to improper sticking of the particles to the surface of stubs. To avoid this problem, the samples containing lead were selected for carbon coating and gold coating to get EDS spectra and SEM micrographs. However one of the samples was gold coated to observe it as secondary electron images (SEI) to get some sharp images. It was rather complicated to locate lead in the gold coated samples as secondary electron images because these images could not differentiate between heavier and lighter elements. However this task can be easily accomplished using back scattered images (BSEI). In order to resolve this problem, the gold coated sample was first observed as BSEI to detect the brighter areas in the sample and after identifying the area, secondary electron image (SEI) mode was turned on to take sharp images of that area.

Lead(II) was found using back scattered image mode as traces in the form of brighter spots in between the grains of synthetic pyroaurite material. The study area measurement (for lead) was also taken into account to get insight that how much area is covered by the heavy metal. The grains containing Pb(II) were scaled. However it is difficult to conclude either the lead was adsorbed on the surface of pyroaurite or it is present in the form of precipitates (Figure 5-27).

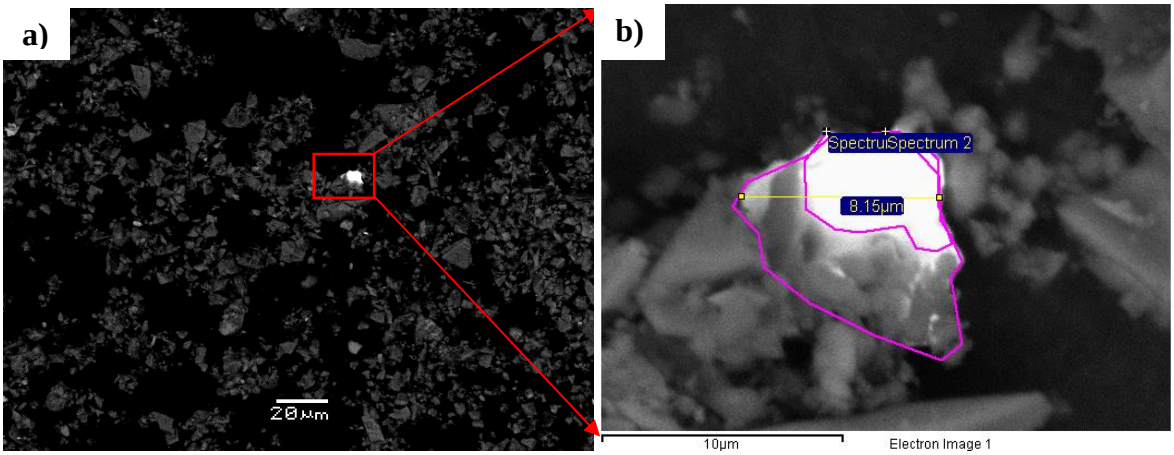

Figure 5-27: Back scattered electron images of selected area in the reacted sample (carbon coated) displaying presence of lead(II). a) The red block indicating the area where lead(II) is located. b) Showing the close-up of the area depicting area of measurement for lead(II).

Spectrum	**O**	**Mg**	**Si**	**Fe**	**Pb**
Spectrum 1	46.00	5.76	14.02	3.87	30.35
Spectrum 2	51.24	7.99	22.17	4.13	14.47
Mean	48.62	6.87	18.09	4.00	22.41
Std. deviation	3.71	1.57	5.76	0.18	11.22
Max.	51.24	7.99	22.17	4.13	30.35
Min.	46.00	5.76	14.02	3.87	14.47

Table 5-6: Quantification of the elements in atomic wt% of the selected area of reacted material in the figure above.

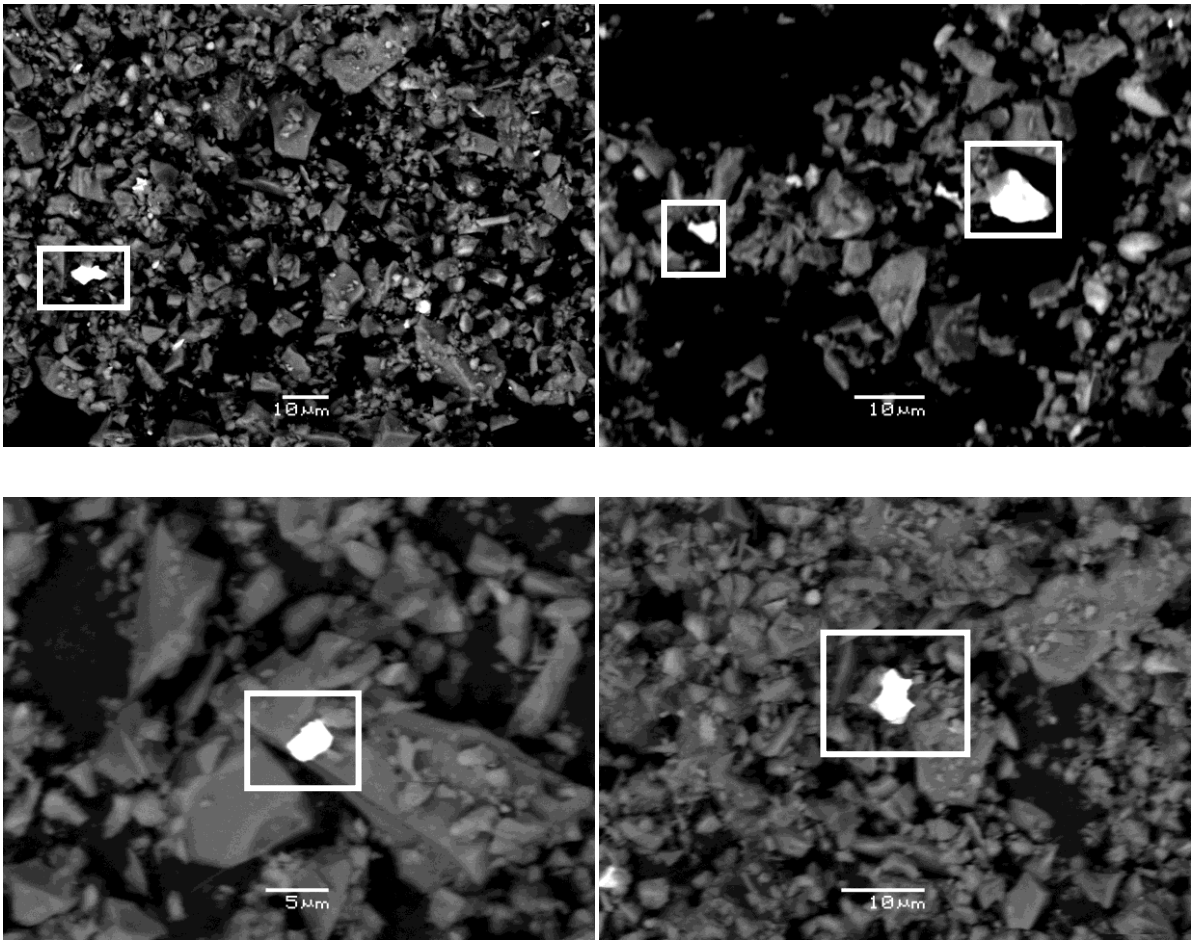

Figure 5-28: Back scattered images of uncoated reacted column material taken at different magnifications at low vacuum. The white boxes highlight the areas containing Pb which is present as a brighter white part.

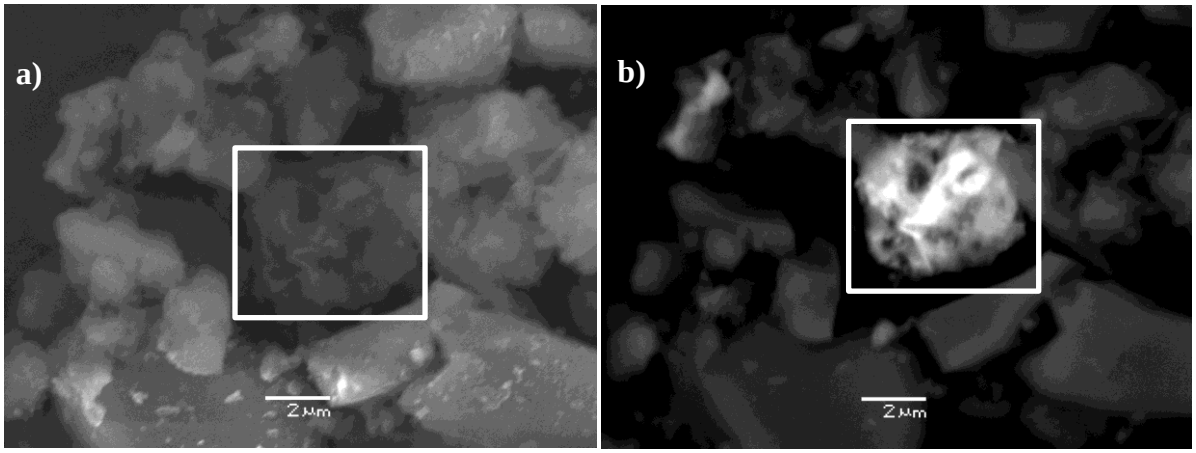

Figure 5-29: Carbon coated sample depicting the structure of lead(II) found in one of the samples. a) The rectangle indicating the area rich in lead in secondary electron image. b) Demonstrates the same area in SEM-BSE image.

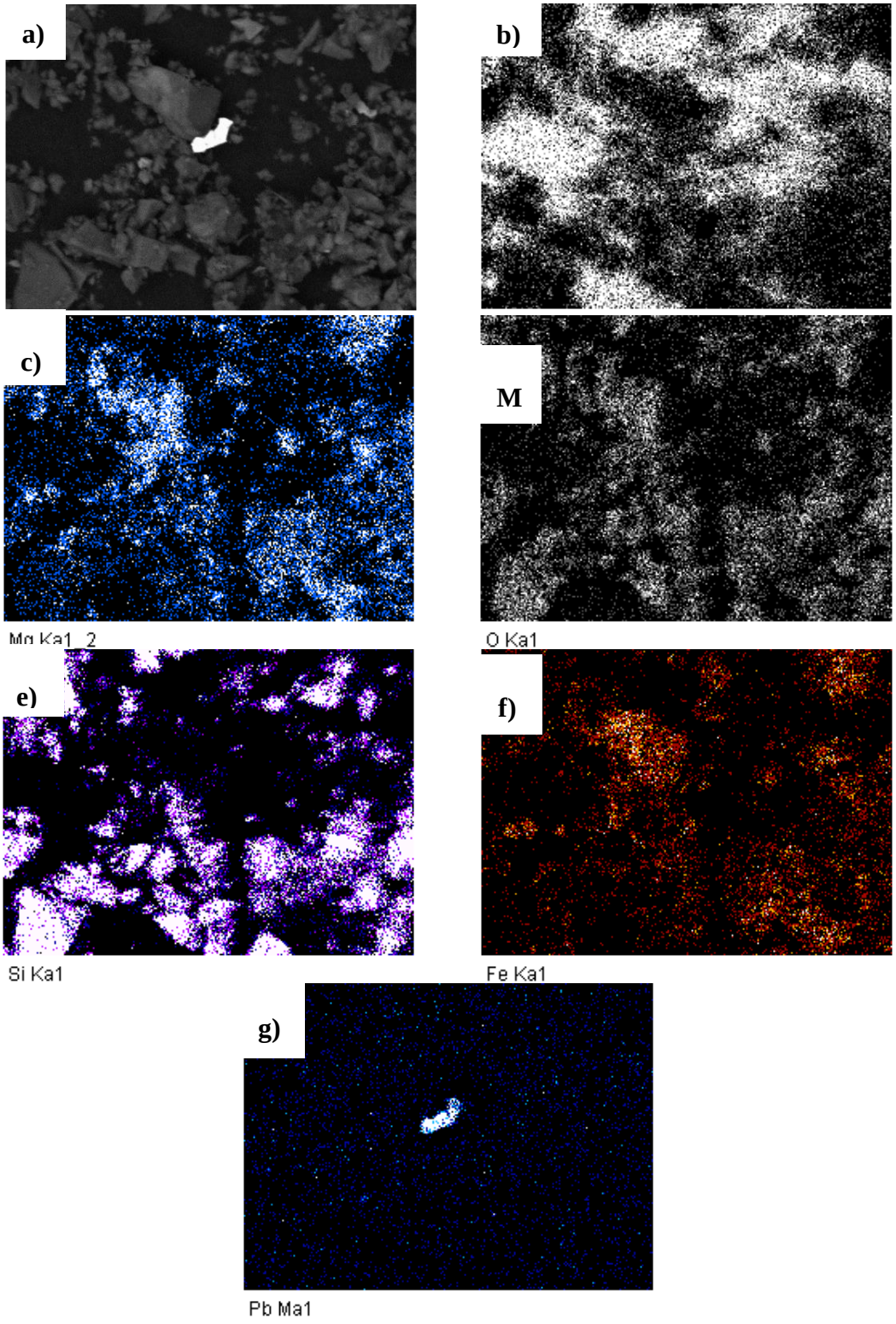

Figure 5-30: Elemental mapping of the carbon coated reacted sample in SEM. a) area selected for mapping b) Map of carbon c) Map of magnesium d) Map of oxygen e) Map of silica f) Map of iron g) Map of lead.

The samples of reacted column material were not coated with carbon or gold on the first hand; however few samples were coated with carbon for further analyses after finding lead in

them. As the pyroaurite material was mixed along with quartz sand, it becomes even more difficult to identify and trace lead(II) in the sample. Lead can be seen as brighter part in the sample by back scattered images because it is a heavy element. Heavy elements displays brighter colour than the lighter elements in BSE images. In our case, it becomes difficult to locate lead in a first glance because titanium and Fe were also present in the sand sample. They also exhibit a brighter colour in BSE images.

Element mapping for the areas of interest have also been done by SEM. Low amounts of lead in the reacted sample makes it difficult to trace. Figure 5-30 shows the elemental mapping of desired area. Here white part or dots in the images represents the highest intensity of the element present in the area. Carbon in Figure 5-30a is mainly due to carbon tape on stub on which the sample was mounted. It can be seen that silica is present all over the selected area of the reacted sample.

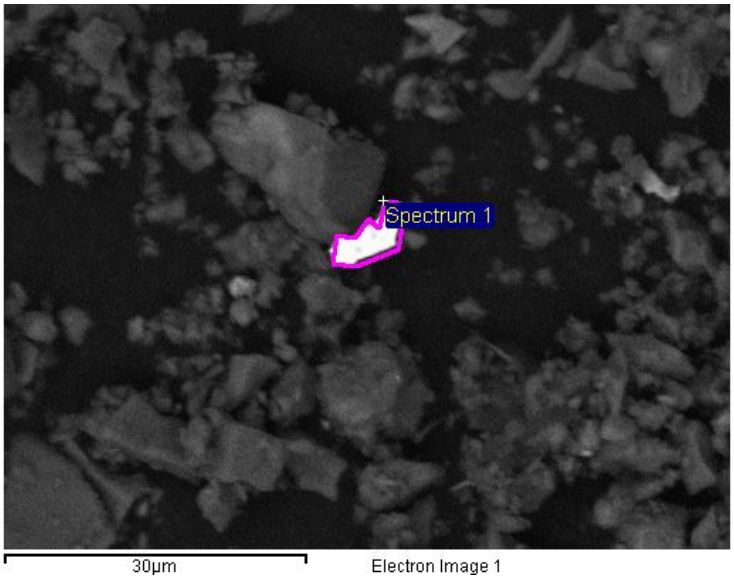

Figure 5-31: SEM-BSE image of the region containing lead. The whole brighter area is selected for EDS spectra and quantification.

Spectrum	O	Si	Pb	Total
Spectrum 1	20.12	3.21	76.67	100
Mean	20.12	3.21	76.67	100
Max.	20.12	3.21	76.67	
Min.	20.12	3.21	76.67	

Table 5-7: Quantification of the chosen area from Figure 5-31 in wt%.

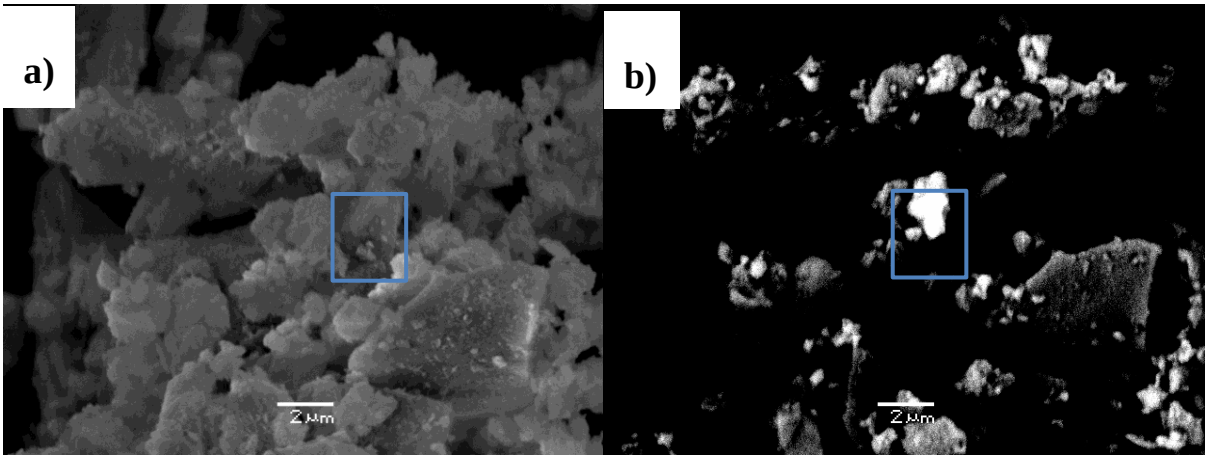

Figure 5-32: a) Displaying the area containing Pb(II) in secondary electron images. b) Highlighting the same area in back scattered electron image.

Table 5-7 demonstrates the elemental quantification of the selected grain in Figure 5-31. In this selected range, oxygen, silicon and lead(II) are present. There are chances that lead oxides might have been formed as no carbon was observed.

Gold coated sample containing lead was also observed as BSEI to identify lead in SEI, which was a demanding task. In BSEI, gold is a heavy element so lot of brighter parts were observed which again makes problematic to locate Pb(II) in the samples. Figure 5-32 highlights the area of the sample comprising Pb(II) in back scattered and secondary electron image. However, in these figures it is not convincing that Pb(II) is in the form of precipitates or either it has adsorbed.

Figure 5-33 exhibits the EDS spectra of the selected field revealing existence of Si, Pb, Fe, Mg and gold (Au) which is added from the coating of the sample.

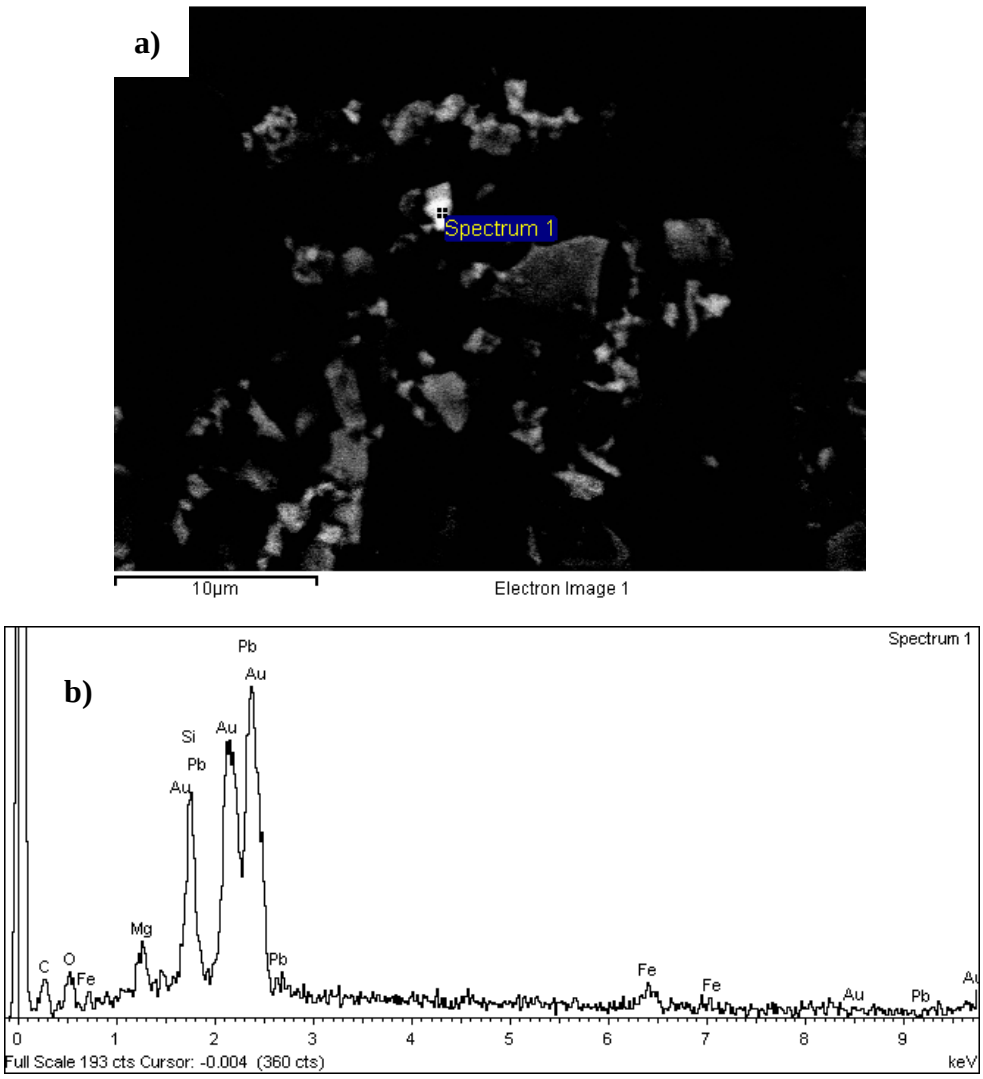

Figure 5-33: a) BSEI of selected area. b) EDS spectra of the image of gold coated sample representing presence of lead (Pb), silica (Si), magnesium (Mg), and iron (Fe).

Figure 5-34 compares the chosen area in SEI and BSEI where lead has incorporated to distinguish between the contrasts of these two modes. In addition, Figure 5-35 exposes the top view of the grain Figure 5-34 in which lead has adsorbed.

Only three samples from both column experiments reveals the presence of lead using SEM These samples are from the top of the column which are nearest to the inlet (Figure 5-22).

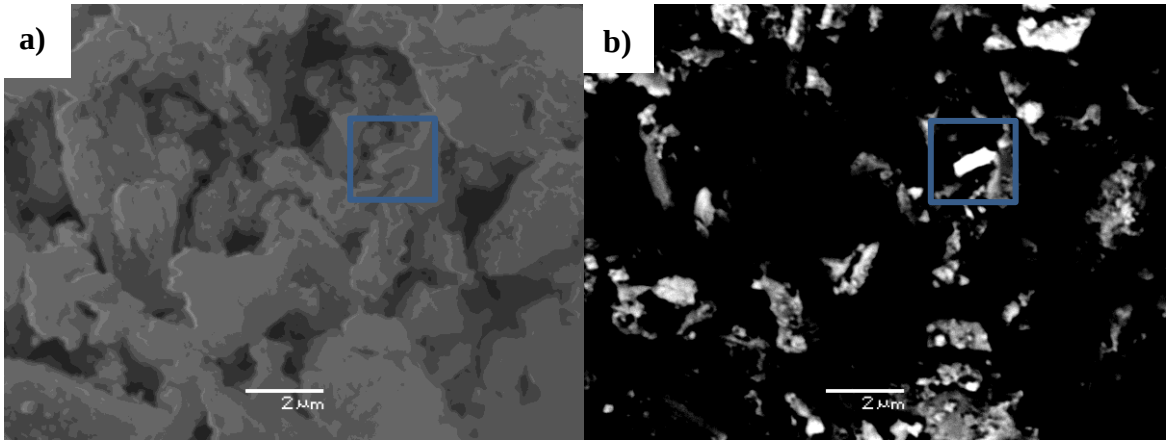

Figure 5-34: Gold coated sample indicating the presence of lead(II) a) in SEI b) in BSEI.

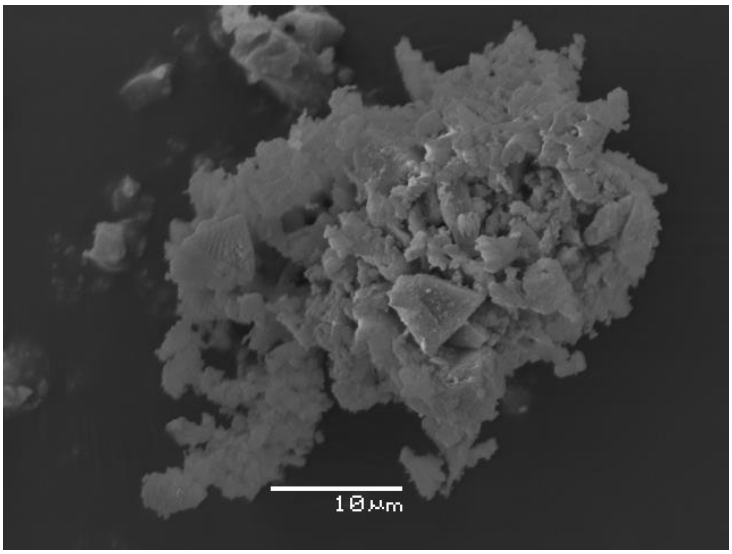

Figure 5-35: Top view of the whole grain shown in Figure 5-34.

6. Discussion

The main purpose of this study is to prepare synthetic pyroaurite in the laboratory and to test its capability to remove Pb^{2+} from $Pb(NO_3)_2$ aqueous solution. Previous studies have revealed that it is possible to remove such heavy metals from waters by using several methods including chemical precipitation, adsorption, and ion- exchange (Naeem et al., 2009).

After conducting the column experiments, the results showed that synthetic pyroaurite-like material has good sorption ability for Pb^{2+} from lead nitrate aqueous solutions specifying that removal of such heavy metal ions is possible.

6.1. Synthetic pyroaurite material

The prepared pyroaurite clay mineral ($Mg_6Fe_2(OH)_{16}(CO_3^{2-}).4H_2O$) is poorly crystalline (Figure 5-1) whereas, it should be crystalline in actual chemistry. The natural pyroaurite mineral has brownish yellow or golden, hexagonal, and platy structure (Taylor, 1973; KOCH, 1991). The reason for the formation of unexpected amorphous form rather than crystalline form could be that while synthesizing the mineral, the solution was not stirred properly as stirring is necessary to get a homogeneous mixture. During titration with NaOH, the solution becomes viscous which makes it difficult to stir at low speed. The solution needs to be stirred overnight, but efficient overnight mixing was not achievable due to lack of an efficient stirrer in the laboratory.

One of the major aspects in crystal formation is the supply of CO_2 during synthesis. The material was prepared in an open beaker so that carbon dioxide will diffuse into the system to form carbonates. But it is difficult to estimate how much CO_2 diffuses into the system during the two days of preparation. Rate of formation of crystals is also dependent upon rate of supply of CO_2. Titration was done with a strong base (NaOH). The strong base serves to increase pH which increases the solubility of CO_2 in water. So indirectly, with increasing solubility, diffusion of CO_2 will also increase.

During the preparation of the material, pH was measured continuously while titrating with sodium hydroxide base (NaOH). The pH for the final solution was about 13.1, but pH was not measured on the next day after the solution was left overnight for stirring. For

confirmation of presence of carbonates in the freshly prepared slurry-like solution, pH should have been measured.

Concentration of dissolved carbonate species depends on pH of the solution. Various carbonate species vary with different pH (Figure 6-1). At pH greater than 10.3, carbonates (CO_3^{2-}) become dominant (Appelo and Postma, 2005). Therefore, pH should be maintained above 10.3 in order to form carbonate crystals. If the pH drops, carbonates will not be formed and if there is excess of CO_2 supply, then the solution will acidify and crystals will start dissolving. Hence, a pH of 13 tends to be quite suitable for the formation of carbonates. During experimentation, when the beaker is left under the atmosphere for one day, pH is unfortunately not measured the next day. On such days, there is uncertainty as to the pH conditions in comparison to the last pH obtained, whether it has been reduced, increased or remains constant. According to De Yoreo and Vekilov (2003), nucleation is the initial stage of crystallization and temperature is one of the factors controlling this process. The size, shape and morphology of the crystals can also be influenced by nucleation.

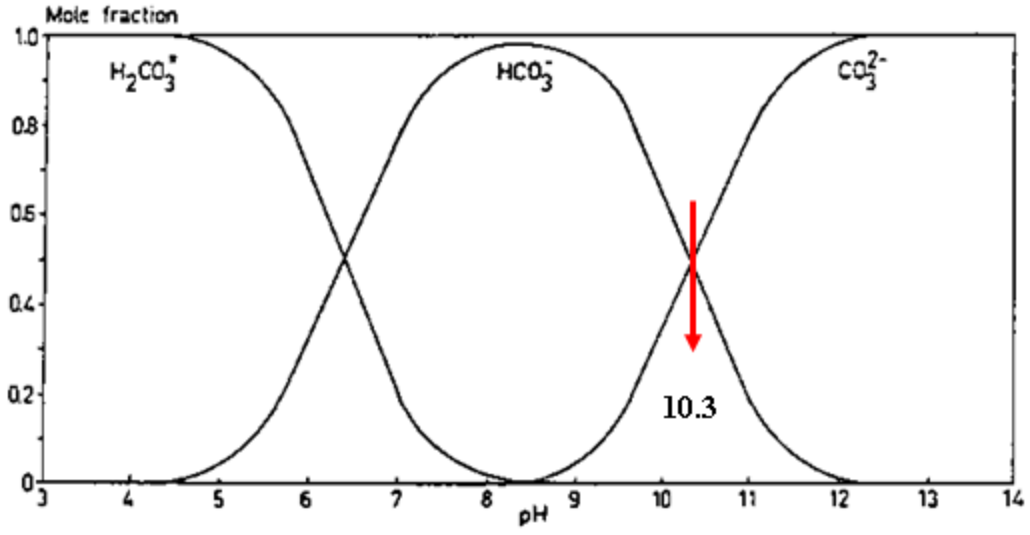

Figure 6-1: Variation of different aqueous carbonate species with pH modified after Appelo and Postma (2005).

Moreover, another unlikely possibility could be that the material was not grinded in a proper manner as crushing of the material was done by hand first. These are the most likely reasons for the poor/no crystal growth.

The formula for pyroaurite ($Mg_6Fe_2(OH)_{16}$ (CO_3^{2-}).$4H_2O$) suggests the presence of higher amounts of magnesium and lower amounts of Fe. However, some anomaly has been found in

our results. From Figure 5-4a and b, it is seen that magnesium (Mg) is higher than iron (Fe) in the sample. But SEM-EDS analysis and quantification of elements exhibits slightly different relation because in some parts Fe is much higher than Mg content (Table 5-1). Presence of secondary phases like brucite and chloromagnesite in considerable amounts (Figure 5-1) supports the fact that Mg is present in higher amounts than Fe.

6.2. Column experiments

Due to lower quantity of prepared clay mineral, the synthetic pyroaurite is accompanied by quartz sand. In my opinion, the pyroaurite material should not be mixed with other materials and large quantities of prepared material should be used in order to avoid different impurities and to get better results.

Pyroaurite has anion as well as cation exchange behaviour. Anions are present in the interlayer region of pyroaurite structure and this can be exchanged by other anions when in contact with negatively charged ions (Liang et al., 2009). The decreasing concentration of nitrate (NO_3^-) in Figure 5-16 and Figure 5-17 supports this fact and proves that synthetic pyroaurite has ability for anion exchange. During the reaction, NO_3^- from $Pb(NO_3)_2$ replaces the hydroxyl (OH^-) and carbonate ions (CO_3^{2-}) from the structure of pyroaurite. These ions are responsible for increasing the pH of the effluent samples (Figure 5-14 and Figure 5-15).

In Figure 5-19, a sudden elevated concentration of Pb(II) has been observed. The most likely reason for this sudden increase might be the discharge and dissolution of a small particle from the column into the effluent samples.

In Figure 5-21, concentration of Mg in the effluent samples decreases with time. It is possible that Mg is released from dissolution of pyroaurite from the sample. Decrease in Mg concentration indicates that the dissolution rate decreases with time. I assume that some of the Mg/Fe released is related to the uptake of Pb, since the co-released CO_3^{2-} will bind to Pb and form $PbCO_3$. Less release of Mg with time may imply that less Pb^{2+} is taken up with the direct precipitation (replacement reaction) with time.

According to World health organization, the standard for the maximum permissible limit of Pb in drinking water is 10 ppb (WHO, 2011). The detected concentration of Pb^{2+} in our samples is far below this drinking water standard as seen in Figure 5-19 and Figure 5-20.

Concentration of Pb^{2+} ranges from 4 to 0.01 ppb. However there is only one sample which exhibit uncertain value showing Pb^{2+} concentration around 14 ppb in Figure 5-19. This is probably due to the column particle which might have migrated and dissolved into the effluent.

6.3. Post experimental solid phase analyses

Investigations from XRD did not exhibit formation of any considerable secondary minerals. XRD can detect changes in the mineralogy (d-spacing) and can also give information of any new phases that may be formed. In this study, it was not possible to detect any secondary phase that contains Pb(II). The possible interpretation could be that the crystallographic structure of pyroaurite in our synthetic samples is not very well defined. In addition, an effect on the d-spacing of any additional Pb in such structure at unknown crystallographic positions is not observed and no sign of presence of any other Pb-bearing phases in the reacted samples is present. This might lead to the conclusion that the Pb detected by the EDS analyses could be due to surface adsorption rather than crystallographic incorporation. The estimated percentage of Pb^{2+} in the 10 gram of column material for experiment one that was run for 8 days and for experiment two that was run for 22 days was only 0.014% and 0.039% respectively.

In SEM-BSE images, the Pb is seen as a brighter part but due to the presence of other minerals in the sand such as quartz and albite, it becomes quite hard to identify Pb. Some impurities probably from the sand are also detected in the samples. The elements Fe, Ti, Zr also appear brighter in back scattered images which make it difficult to distinguish between them and Pb. Due to this reason, longer period of time has been spent in detecting lead in all the samples. A suggested solution to this problem would be the use of only pure quartz sand rather than the use of mixed sand. Another solution could be the use of only pure synthesized pyroaurite mineral in the column experiments. This way, there may be a better chance of getting clearer results. To analyse the actual chemistry of reacted samples, the samples were not coated. This creates some difficulties as some of the grains were loosely bind and not sitting properly on the stubs. So sometimes the required grain vanished when hit by the electron beam for observation. However, one of the reacted samples was gold coated in order to obtain sharp images. As secondary electron images are required for gold coated samples, it

was difficult to differentiate between the elements in SEI unlike in BSE images where it was easier to identify and differentiate between heavy and light elements.

Lead(II) is found in different locations of the samples. The expectation was to get Pb(II) adsorbed all over the synthesized pyroaurite mineral but the outcome is not as expected. Lead is found in several areas of the rounded sample and it appears as some brighter white spots or sometimes as brighter particles in BSEI. It will be accurate to say that the heavy metal Pb is not much sorbed but it has been seen as precipitates on synthetic pyroaurite material. According to Godelitsas and Astilleros (2010) Pb can be precipitated on surfaces having CO_3^{2-} substrate by forming a new Pb phase minerals like cerussite ($Pb(CO_3)$).

In addition, instead of analysing stub mounted samples, thin sections of the reacted solid should be prepared and observed. Flat samples usually gave better results in SEM whereas in stub mounted samples, grain particle lie on top of each other, thus having irregular pattern which sometimes makes it a little problematic to observe exact amount and composition of the sample. SEM images shows topography of the samples and the observed Pb tends to be in small amounts. It therefore, may be possible that either lead(II) is actually present in small quantities or it could be present in the form of thin coatings on the pyroaurite.

It is estimated that about 99% of lead(II) is immobilized into the synthetic pyroaurite material through sorption mechanism. The experiments were run twice. The similar results from both experiments complement each other and suggested the similar mechanisms responsible for the removal of lead(II) from the aqueous solutions. It is hard to conclude that the Pb(II) is either forming precipitates or adsorbing on the pyroaurite material. Further analyses are required to confirm the dominant mechanisms through which the Pb(II) is being taken up by the synthetic pyroaurite. Desorption experiments can be conducted to validate if adsorption had actually played a role in the uptake of Pb(II).

7. Summary and conclusions

This study is based upon experimental work and analysis in order to determine the potential of synthetic pyroaurite mineral for the removal of heavy metal lead (Pb^{2+}) from contaminated water using column experiments. The experiments are conducted twice in order to test for consistency in reactions, to gain full understanding and to confirm the potential of pyroaurite-like compound for the removal of Pb^{2+}.

Pyroaurite-like compound was synthesized in the laboratory under ordinary room temperature. This prepared material was then characterized to determine its structure and mineral composition using XRD and SEM. The result reveals that poorly crystalline pyroaurite mineral was formed. This material was then used to perform column experiments to test the capability of synthetic pyroaurite for removal of Pb^{2+} from $Pb(NO_3)_2$ aqueous solutions. Synthesized pyroaurite was mixed with finely grained natural sand to achieve better flow properties of column. Inlet solution of 10 mg $Pb(NO_3)_2$ was prepared to pump through the column at flow rate of 1.25 ml/hour. Liquid samples were collected for each column experiment to measure the concentration of lead and magnesium using ICP-MS.

Results from duplicates were quite similar. Concentration of lead in outlet samples is far lower than the inlet solution lead(II) concentrations; showing that 99% of the lead has been removed. The effluent concentration is also far below the provisional drinking water standard put forward by WHO (2012) of 10 microgram/liter, reaching as low as 0.1-0.2 microgram/liter after a few days. The reacted solid column material was also analysed by XRD and SEM to see if any changes in mineralogy and or sign of lead enrichment could be detected. Traces of lead were found while analysing under scanning electron microscope. Lead was detected in minute particles in some samples, while in others no traces of Pb could be seen. Characterization of reacted material in XRD did not reveal formation of secondary Pb-phases. It should be noted that the total amount of lead scavenged, is below detection limit of XRD.

On the basis of all the observations and analysis from various analytical techniques, it can be concluded that almost all of the incoming lead(II) is taken up by the synthetic pyroaurite material. Although the exact mechanism for uptake of Pb^{2+} is not quite clear, lead(II) has either been adsorbed/ions exchange on the surface of pyroaurite material or precipitated as a

new mineral phase. These two processes, i.e. adsorption/ion exchange and precipitation, seem to play important roles in the immobilization of lead(II). The solid-phase analyses indicate that lead is concentrated at few spots in the sample giving an indication of formation of a secondary Pb phase; probably lead carbonate $Pb(CO_3)$ or lead oxide. On the other hand, sorption is difficult to observe, but it is likely to be responsible for some of the Pb-uptake.

The main conclusion from this study is that pyroaurite-like material has proved to be an effective sorbent in removal of Pb(II) from aqueous solution of $Pb(NO_3)_2$. The sorption process is able to meet the guideline values defined by WHO.

Recommendations for future work

- The satisfactory results from this study have brought up many considerable approaches for further investigations. As the synthetic pyroaurite has proven to be efficient in removal of lead(II) from aqueous solution, further work in this regard needs to be done.
- Synthetic pyroaurite should be tested for the removal of other heavy metal pollutants like cadmium, copper and others.
- Column experiments can be performed using different concentrations of lead in aqueous solutions to determine if synthetic pyroaurite has potential to immobilize higher amounts of lead. The experiments should be performed with the prepared synthetic pyroaurite material solely, or it should be accompanied with pure quartz sand rather than poly-mineralic sands. The reaction time can be increased further for investigation of the mechanism by which lead(II) is taken up by pyroaurite. In addition, experiments can be performed with higher amounts of lead(II) in the waters. This way results will be more clear and evident.
- Computer modelling for sorption behaviour and transport of heavy metals can also be implemented.
- To get clear results for tracing the heavy metal into the pyroaurite structure, thin sections should be prepared for analysing the reacted samples. For detailed analysis and observation of samples, more efficient analytical techniques should be utilized.

References

Adelekan, B. and Abegunde, K., (2011). Heavy metals contamination of soil and groundwater at automobile mechanic villages in Ibadan, Nigeria. Int. J. Phys. Sci, **6**(5): p. 1045-1058.

Allmann, R., (1968). The crystal structure of pyroaurite. Acta Crystallographica Section B: Structural Crystallography and Crystal Chemistry, **24**(7): p. 972-977.

Alyüz, B. and Veli, S., (2009). Kinetics and equilibrium studies for the removal of nickel and zinc from aqueous solutions by ion exchange resins. Journal of hazardous materials, **167**(1): p. 482-488.

Appelo, C. A. J. and Postma, D., (2005). Geochemistry, groundwater and pollution, CRC Press.

Bailey, S. E., Olin, T. J., Bricka, R. M. and Adrian, D. D., (1999). A review of potentially low-cost sorbents for heavy metals. Water Research, **33**(11): p. 2469-2479.

Baltpurvins, K., Burns, R., Lawrance, G. and Stuart, A., (1997). Effect of electrolyte composition on zinc hydroxide precipitation by lime. Water Research, **31**(5): p. 973-980.

Barakat, M., (2011). New trends in removing heavy metals from industrial wastewater. Arabian Journal of Chemistry, **4**(4): p. 361-377.

Beinlich, A. and Austrheim, H., (2012). In situ sequestration of atmospheric CO2 at low temperature and surface cracking of serpentinized peridotite in mine shafts. Chemical Geology, **332–333**(0): p. 32-44.

Blöcher, C., Dorda, J., Mavrov, V., Chmiel, H., Lazaridis, N. K. and Matis, K. A., (2003). Hybrid flotation - Membrane filtration process for the removal of heavy metal ions from wastewater. Water Research, **37**(16): p. 4018-4026.

Bruun Hansen, H. C. and Koch, C. B., (1995). Synthesis and characterization of pyroaurite. Applied Clay Science, **10**(1): p. 5-19.

Burgess, J., (1999). Ions in solution: basic principles of chemical interactions, Elsevier.

Corporation, D., (2006). ICS-2000 Ion Chromatography System Operator's Manual.

Dabrowski, A., Hubicki, Z., Podkościelny, P. and Robens, E., (2004). Selective removal of the heavy metal ions from waters and industrial wastewaters by ion-exchange method. Chemosphere, **56**(2): p. 91-106.

De Yoreo, J. J. and Vekilov, P. G., (2003). Principles of crystal nucleation and growth. Reviews in mineralogy and geochemistry, **54**(1): p. 57-93.

Dean, J. G., Bosqui, F. L. and Lanouette, K. H., (1972). Removing heavy metals from waste water. Environmental Science & Technology, **6**(6): p. 518-522.

Diouf, R., Ndiaye, S. and Muhr, L., (2011). Adsorption in column of Cu (II), Ni (II) and Pb (II) with XAD-7 resin impregnated with bis (2-ethylhexyl) ammonium bis (2-ethylhexyl) dithiocarbamate (BEABEDC) in aqueous solution. Int. J. Phys. Sci, **6**(13): p. 3263-3269.

Egila, J., Dauda, B., Iyaka, Y. and Jimoh, T., (2011). Agricultural waste as a low cost adsorbent for heavy metal removal from wastewater. Int J Phys Sci, **6**(8): p. 2152-2157.

Forano, C., (2004). Environmental remediation involving layered double hydroxides, Elsevier: New York.

Fu, F. and Wang, Q., (2011). Removal of heavy metal ions from wastewaters: a review. Journal of Environmental Management, **92**(3): p. 407-418.

Gode, F. and Pehlivan, E., (2006). Removal of chromium (III) from aqueous solutions using Lewatit S 100: the effect of pH, time, metal concentration and temperature. Journal of hazardous materials, **136**(2): p. 330-337.

Godelitsas, A. and Astilleros, J. M., (2010). Dissolution, sorption/(re) precipitation, formation of solid solutions and crystal growth phenomena on mineral surfaces: implications for the removal of toxic metals from the environment. EMU Notes in Mineralogy, **10**: p. 289-324.

Hansen, H. C. B. and Taylor, R., (1990). Formation of synthetic analogues of double metal-hydroxy carbonate minerals under controlled pH conditions: I. The synthesis of pyroaurite and reevesite. Clay Minerals, **25**(2): p. 161-179.

Huisman, J. L., Schouten, G. and Schultz, C., (2006). Biologically produced sulphide for purification of process streams, effluent treatment and recovery of metals in the metal and mining industry. Hydrometallurgy, **83**(1): p. 106-113.

Igwe, J. C., Okpareke, O. C. and Abia, A. A., (2006). Removeal of Co (Ii), Fe (Ii) and Cu (Ii) ions from wasterwater using modified and unmodified maize husk: Sorption kinetics and intraparticulate diffusivity. European Journal of Scientific Research, **13**(2): p. 206-212.

Jaiswal, A. and Chattopadhyaya, M., (2011). Interaction of Mn2+, Fe2+ and Cu2+ heavy metal ions from aqueous solution by zaccagnaite, a hydrotalcite-like compound. Desalination and Water Treatment, **29**(1-3): p. 252-257.

Jayakumar, R., Menon, D., Manzoor, K., Nair, S. and Tamura, H., (2010). Biomedical applications of chitin and chitosan based nanomaterials—A short review. Carbohydrate Polymers, **82**(2): p. 227-232.

Järup, L., (2003). Hazards of heavy metal contamination. British medical bulletin, **68**(1): p. 167-182.

Kim, J. S., Akeprathumchai, S. and Wickramasinghe, S. R., (2001). Flocculation to enhance microfiltration. Journal of Membrane Science, **182**(1-2): p. 161-172.

KOCH, C. B., (1991). On the genesis and composition of natural pyroaurite. Clay Minerals, **26**: p. 297-309.

Koch, C. B., (1998). Structures and properties of anionic clay minerals. Hyperfine Interactions, **117**(1-4): p. 131-157.

Kruissink, E. C., van Reijen, L. L. and Ross, J. R., (1981). Coprecipitated nickel–alumina catalysts for methanation at high temperature. Part 1.—Chemical composition and structure of the precipitates. Journal of the Chemical Society, Faraday Transactions 1: Physical Chemistry in Condensed Phases, **77**(3): p. 649-663.

Kurniawan, T. and Babel, S., (2003). A research study on Cr (VI) removal from contaminated wastewater using low-cost adsorbents and commercial activated carbon. Second Int. Conf. on Energy Technology towards a Clean Environment (RCETE).

Leung, W., Wong, M., Chua, H., Lo, W., Yu, P. and Leung, C., (2000). Removal and recovery of heavy metals by bacteria isolated from activatedsludge treating industrial effluents and municipal wastewater. Water Science & Technology, **41**(12): p. 233-240.

Liang, X., Hou, W. and Xu, J., (2009). Sorption of Pb (II) on Mg‑Fe Layered Double Hydroxide. Chinese Journal of Chemistry, **27**(10): p. 1981-1988.

Liang, X., Zang, Y., Xu, Y., Tan, X., Hou, W., Wang, L. and Sun, Y., (2013). Sorption of metal cations on layered double hydroxides. Colloids and Surfaces A: Physicochemical and Engineering Aspects, **433**: p. 122-131.

Longerich, H., Jenner, G., Fryer, B. and Jackson, S., (1990). Inductively coupled plasma-mass spectrometric analysis of geological samples: a critical evaluation based on case studies. Chemical Geology, **83**(1): p. 105-118.

Lundh, M., Jönsson, L. and Dahlquist, J., (2000). Experimental studies of the fluid dynamics in the separation zone in dissolved air flotation. Water Research, **34**(1): p. 21-30.

Lützenkirchen, J., (2002). Surface complexation models of adsorption: a critical survey in the context of experimental data. Surfactant science series, **107**: p. 631-710.

Miyata, S., (1983). Anion-exchange properties of hydrotalcite-like compounds. Clays Clay Miner, **31**(4): p. 305-311.

Naeem, A., Saddique, M., Mustafa, S., Kim, Y. and Dilara, B., (2009). Cation exchange removal of Pb from aqueous solution by sorption onto NiO. Journal of hazardous materials, **168**(1): p. 364-368.

Naiya, T. K., Bhattacharya, A. K. and Das, S. K., (2009). Adsorption of Cd (II) and Pb (II) from aqueous solutions on activated alumina. Journal of colloid and interface science, **333**(1): p. 14-26.

Rashed, M., (2001). Lead removal from contaminated water using mineral adsorbents. Environmentalist, **21**(3): p. 187-195.

Reed, B. E., Carriere, P. C. and Moore, R., (1996). Flushing of a Pb (II) contaminated soil using HCl, EDTA, and CaCl2. Journal of Environmental Engineering, **122**(1): p. 48-50.

Reed, S. J. B., (2005). Electron microprobe analysis and scanning electron microscopy in geology, Cambridge University Press Cambridge.

Reichle, W. T., (1986). Synthesis of anionic clay minerals (mixed metal hydroxides, hydrotalcite). Solid State Ionics, **22**(1): p. 135-141.

Seida, Y. and Nakano, Y., (2000). Removal of humic substances by layered double hydroxide containing iron. Water Research, **34**(5): p. 1487-1494.

Seida, Y., Nakano, Y. and Nakamura, Y., (2001). Rapid removal of dilute lead from water by pyroaurite-like compound. Water Research, **35**(10): p. 2341-2346.

Seiler, H., Sigel, A. and Sigel, H., (1994). Handbook on metals in clinical and analytical chemistry, CRC Press.

Setshedi, K., Ren, J., Aoyi, O. and Onyango, M. S., (2012). Removal of Pb (II) from aqueous solution using hydrotalcite-like nanostructured material. Int. J. Phys. Sci, **7**: p. 63-72.

Sobolev, D. and Begonia, M., (2008). Effects of heavy metal contamination upon soil microbes: lead-induced changes in general and denitrifying microbial communities as evidenced by molecular markers. International journal of environmental research and public health, **5**(5): p. 450-456.

Sparks, D. L., (2003). Environmental soil chemistry, Academic press.

Stevenson, F. J., (1994). Humus chemistry: genesis, composition, reactions, John Wiley & Sons.

Suryanarayana, C. and Norton, M. G., (1998). X-ray diffraction: a practical approach, Springer.

Taylor, H., (1973). Crystal structures of some double hydroxide minerals. Mineral. Mag, **39**(304): p. 377-389.

Thomas, R., (2013). Practical guide to ICP-MS: a tutorial for beginners, CRC press.

Wang, L. K., Hung, Y.-T. and Shammas, N. K., (2005). Physicochemical treatment processes, Springer.

Weiner, E. R., (2012). Applications of environmental aquatic chemistry: a practical guide, CRC Press.

Weiss, J., (2008). Ion chromatography, John Wiley & Sons.

WHO, (2011). Guidelines for drinking-water quality - 4th ed, World Health Organization.

Appendices

Appendix 1a: calculation for converting lead concentration into ppm.

Molar mass of $Pb(NO_3)_2$= 331.2 g/mol → 0.3312 g/L = 1 mmol/l

1 mmol/l → molecular wt. (lead) 207.2 / 331.2 = 0.63 ppm

1gram $Pb(NO_3)_2$ = 0.63 gram of Pb(II)

1ppm = 10^{-6} g

1g $Pb(NO_3)_2$ / L =630 ppm

10 mg $Pb(NO_3)_2$ /L = 6.3 ppm

Appendix 1b

For column 1:

Δ Pb = $C_{Pb(solution)}.V_{total}$

For column 1: 4 gram of pyroaurite and 6 gram of natural sand were used

Time: 8 days ; flow rate through column : 1.25 ml/hour

8days * 24 = 192

192 * 1.25 = 240 ml (total volume of water used9

Incoming lead: 5.85 mg/l,

Putting values in equation:

5.85 * 0.240 = 1.4 mg Pb (10 g total amount of material sand +clay)

1.4/10,000 = 0.00014 = 0.014%

For column 2: 4 gram of pyroaurite and 6 gram of natural sand were used.

$\Delta Pb = C_{Pb(solution)}.V_{total}$

Time: 22 days; flow rate through column: 1.25 ml/hour

22 days * 24 = 528

528 * 1.25 = 660 ml

Now, putting values in equation:

528 * 0.660 = 3.861 mg Pb^{2+}

3.861/ 10,000 = 0.0003861 = 0.039%

APPENDIX 2:

Table A: Measured pH of samples from first column.

Column T-1	pH	Time (hour)
s-original	6.5	0
s-21	9.2	1
s-22	9.1	2
s-23	8.5	3
s.24	8.9	4
s-25	9.1	5
s-26	9	6
s-27	8.8	7
s-28	8.72	8

Table B: Measured pH of samples from second column

Column T-2	pH	Time(d)
Original	6.5	0
sample 12	9.3	2
sample15	9.2	2.5
sample17	9.3	4
sample27	8.5	6
sample32	8.62	7
sample34	8.45	8
sample37	8.5	9
sample38	8.5	11
sample39	8.81	12
sample40	8.8	13
sample42	8.4	14
sample44	8.6	15
sample45	8.83	16

Table C: Anion Detection using IC (Trial 1)

Sample	Time	Amount	Amount	Amount
Orig. inlet soln.	1	2.05	0.44	3.60
Orig. 21	3	0.97	0.84	2.69
Orig. 24	4	0.72	0.66	2.59
Orig. 25	5	0.58	0.55	2.53
Orig. 26	6	0.55	0.49	2.43
Orig. 27	7	0.51	0.49	2.42
Orig. 28	8	0.49	0.49	2.41
Orig. 29	9	0.48	0.48	2.32

Table D: Anion detection using IC. (Trial 2)

Sample	Time	Amount	Amount	Amount
T2 orig		1.82	0.46	3.86
T2 orig. 12	2 hour	3.41	2.96	2.90
T2 orig. 13	4 hour	1.19	1.83	2.68
T2 orig. 14	6 hour	1.04	1.58	2.68
T2 orig. 15	8 hour	1.65	1.19	2.61
T2 orig. 16	10 hour	0.66	0.90	2.50
Orig. 17	(DAYS) 7	0.39	0.22	2.50
Orig. 32	8	0.32	0.07	2.21
Orig. 33	9	0.48	0.08	2.11
Orig. 34	10	0.30	0.06	2.11
Orig. 35	11	0.22	0.04	2.07
Orig. 37	12	0.29	0.05	2.00
Orig. 38	13	0.28	0.04	1.90
Orig. 39	14	0.26	0.05	1.90
Orig. 40	15	0.26	0.03	1.86
Orig. 41	16	0.33	0.03	1.81
Orig. 42	17	0.24	0.04	1.90
Orig. 43	18	0.36	0.03	1.90
Orig. 44	19	0.18	0.03	1.97
Orig. 45	20	0.17	0.03	2.16

Table E: Concentration of lead(II) in effluent from trial one.

Samples	Conc.(ppb)	Pore volume	Cum.V	Pb %RSD	ERROR ppb
Sample1	2.56	0.25	0.8	2.4	0.061457
Sample2	0.13	0.5	1.6	4.85	0.006135
Sample3	0.21	0.74	2.4	3.57	0.007397
Sample4	0.65	0.99	3.2	1.76	0.011459
Sample5	4.14	1.24	4	1.29	0.053387
Sample6	14.86	1.49	4.8	0.77	0.114451
Sample7	0.65	1.73	5.6	1.84	0.012017
Sample8	0.45	1.98	6.4	2.96	0.013208
Sample9	0.87	2.23	7.2	2.06	0.017957
Sample10	0.46	2.476	8	2.9	0.013331
Sample11	0.14	2.74	8.8	2.75	0.003985
Sample12	0.08	3.22	10.4	6.68	0.005384
Sample13	0.06	3.5	11.27	8.31	0.004712
Sample14	0.08	3.75	12.1	7.3	0.005716
Sample15	0.10	4	12.9	4.54	0.004413
Sample16	0.07	4.24	13.7	7.31	0.005249
Sample17	0.05	4.5	14.5	7.62	0.003635
Sample18	0.06	4.74	15.3	5.38	0.003163
Sample19	0.07	5.01	16.2	5.43	0.003633
Sample20	0.15	5.3	17	2.23	0.003289
Sample21	0.04	5.51	17.8	4.52	0.002011
Sample22	0.19	5.75	18.6	2.6	0.004867
Total	**26.07**				

Table F: Concentration of lead(II) in effluent from second trial.

Samples	Pb (ppb)	Pb	Error ppb	Pore Volume
Sample1	0.63	1.7	0.010792	0.25
Sample2	0.53	2.18	0.011661	0.5
Sample3	0.10	4.91	0.004763	0.74
Sample4	0.10	5.98	0.006004	0.99
Sample5	0.24	3.37	0.00792	1.24
Sample6	0.31	2.02	0.006294	1.49
Sample7	0.23	2.73	0.006361	1.73
Sample8	0.20	3.41	0.006922	1.98
Sample9	0.17	3.34	0.005615	2.23
Sample10	0.16	3.49	0.005539	2.48
Sample12	0.11	4.54	0.005176	2.72
Sample15	0.11	5.12	0.005427	2.97
Sample16	0.0452	5.56	0.002513	3.219814
Sample16	0.0452	5.56	0.002513	3.591331
Sample17	0.0741	4.52	0.003349	3.978328
Sample18	0.1302	2.52	0.003281	4.365325
Sample19	0.0455	5.88	0.002675	4.752322
Sample20	0.0373	7.77	0.002898	5.139319
Sample21	0.02	9.08	0.001816	5.526316
Sample22	0.0181	8.58	0.001553	5.913313
Sample23	0.0166	11.16	0.001853	6.30031
Sample24	0.0462	4.01	0.001853	6.687307
Sample25	0.0279	7.32	0.002042	7.074303
Sample26	0.0288	7.08	0.002039	7.4613
Sample27	0.0158	15.26	0.002411	7.848297

Sample28	0.0187	49.06	0.009174	8.235294
Sample29	0.0131	14.16	0.001855	8.622291
Sample30	0.016	9.98	0.001597	9.009288
Sample31	0.0213	7.64	0.001627	9.396285
Sample32	0.0167	11.94	0.001994	9.783282
Sample33	0.0143	10.68	0.001527	10.17028
Sample34	0.015	10.56	0.001584	10.55728
Sample35	0.0158	12.15	0.00192	10.94427
Sample36	0.0594	3.03	0.0018	11.33127
Total	**4.2**			

Table G: Concentration of magnesium in effluent samples.

Sample	ppb Mg Conc.	%RSD	Time (Hours)
Sample16	181.84	1.76	
Sample 18	48.80	5.19	1
Sample 22	50.30	4.79	2
Sample 23	41.80	2.36	3
Sample 27	33.59	8.02	4
Sample 29	29.51	6.58	5
Sample 30	28.50	4.53	6
Sample 31	39.53	4.4	7
Sample 32	26.39	6.53	8
Sample 33	20.78	7.55	9
Sample 34	20.79	5.39	10
Sample 35	18.51	4.41	11
Sample 37	14.84	4.15	12
Sample 38	9.74	5.03	13
Sample 39	8.63	3.05	14
Sample 40	7.78	10.83	15
Sample 41	6.76	6.28	16
Sample 42	6.81	13.08	17